PMFSEL REPORT NO. 06-01

April 2006

Investigation of the Vibrations on Overhead Sign Bridges on US290/SH71

by

Eric Schell

Liang Yu

Karl H. Frank

conducted for the

Texas Department of Transportation

Investigation of the Vibrations on Overhead Sign Bridges on US290/SH71

FINAL REPORT

Prepared for the

Texas Department of Transportation

Eric Schell

Liang Yu

Karl H. Frank

and

Chris Tessler

Department of Civil Engineering

The University of Texas at Austin

April 2006

Table of Contents

SUMMARY **1**

CHAPTER 1: INTRODUCTION AND INSPECTION OF SIGN SUPPORTS **3**

1.1 Overview of Field Studies 4
1.2 Analytical Studies 5
1.3 Examination of Sign and Supports from OSB-W 5

CHAPTER 2: FIELD TEST RESULTS **9**

2.1 Overview of Field Tests 9
2.2 OSB Natural Frequencies of Vibration—Pluck Test 9
2.3 OSB Acceleration Data from Traffic Loads 11
2.3.1 OSB-E Acceleration Data *12*
2.3.2 OSB-W Acceleration Data *13*
2.4 Highway Bridge Mode Shapes 14
2.5 Highway Bridge and OSB Vibration Analysis 16
2.6 Displacement Measurements Using Video Images 20
2.6.1 Video Measurement Method *21*
2.6.2 Video Data Results *21*
2.7 OSB-E Stain Gage Data and Fatigue Life Estimate 23
2.7.1 OSB-E Strain Time-Series Data *23*
2.7.2 OSB-E Long Term Rainflow Analysis *23*

CHAPTER 3: ANALYTICAL INVESTIGATION OF THE VIBRATIONS ON OVERHEAD SIGN BRIDGE **27**

3.1 Geometry of Overhead Sign Bridges 27
3.1.1 Detailed Geometry of OSB-E at Station 10633+00 ..... *28*
3.1.2 Detailed Geometry of OSB-W at Station 10625+15 ..... *29*
3.1.3 Material Properties *31*
3.2 Analysis of OSB-E 31
3.2.1 Natural Frequency Analysis *31*
3.2.2 Increase of Member Size *33*
3.2.3 Pluck Test Simulation *33*
3.2.4 Dynamic Response Analysis *34*
3.2.5 Dynamic Response Analysis without the Horizontal Arms of Sign Frame *36*
3.3 Analysis of OSB-W 38
3.3.1 Natural Frequency Analysis *38*
3.3.2 Dynamic Response Analysis *39*
3.3.3 Dynamic Response Analysis without the Horizontal Arms of Sign Frame *40*

CHAPTER 4: SUMMARY AND RECOMMENDATIONS **43**

4.1 Summary 43
4.2 Recommendations 43

APPENDIX A: MODEL SHAPES OSB-E **45**

APPENDIX B: MODE SHAPES OSB-W **51**

List of Figures

FIGURE 1.1 OVERHEAD SIGN BRIDGES INVESTIGATED 4
FIGURE 1.2 HORIZONTAL LEG OF L FRAME 6
FIGURE 1.3 CRITICAL FATIGUE DETAIL 6
FIGURE 1.4 FRETTING AND RUST STAINING ON VERTICAL SUPPORTS 7
FIGURE 2.1 PLUCK TEST RESULTS OSB-E 10
FIGURE 2.2 PLUCK TEST RESULTS OSB-W 11
FIGURE 2.3 LOCATION INSTRUMENTATION ON OSB 12
FIGURE 2.4 HORIZONTAL VIBRATION OF OSB-E 13
FIGURE 2.5 OSCILLATIONS OF OSB-W 14
FIGURE 2.6 ACCELERATIONS AND DISPLACEMENTS OF BRIDGE DECK AT OSB-E 15
FIGURE 2.7 BENDING AND TORSIONAL OSCILLATIONS OF OSB-E 16
FIGURE 2.8 HIGHWAY BRIDGE DECK ACCELERATION SPECTRUM AT OSB-E 17
FIGURE 2.9 HIGHWAY BRIDGE DECK ACCELERATION SPECTRUM AT OSB-W 17
FIGURE 2.10 HORIZONTAL RESPONSE OF OSB-E TO VERTICAL BRIDGE VIBRATION 18
FIGURE 2.11 VERTICAL RESPONSE OF OSB-E TO VERTICAL BRIDGE VIBRATION 19
FIGURE 2.12 VERTICAL RESPONSE OF OSB-W TO VERTICAL BRIDGE VIBRATION 20
FIGURE 2.13 COMPARISON OF DISPLACEMENT FROM VIDEO AND ACCELERATION DATA OSB-E 22
FIGURE 2.14 SUPPORT BRACKET WELD DETAIL 25
FIGURE 3.1 STANDARD DESIGN OF OVERHEAD SIGN BRIDGE 27
FIGURE 3.2 SCHEMATIC OF OSB-E STRUCTURAL MODEL 28
FIGURE 3.3 SIGN AND SIGN SUPPORT LAYOUT OSB-E 29
FIGURE 3.4 SCHEMATIC OF OSB-W STRUCTURAL MODEL 30
FIGURE 3.5 SIGN AND SIGN SUPPORT LAYOUT OSB-W 30
FIGURE 3.6 ABAQUS MODELS-(A) OSB 10633 MODEL; (B) HIGHWAY BRIDGE MODEL; (C) OSB 10633 AND HIGHWAY BRIDGE MODEL 31
FIGURE 3.7 FIELD PLUCK TEST RESULTS 33
FIGURE 3.8 ABAQUS SIMULATED PLUCK TEST RESULTS 34
FIGURE 3.9 TIME SERIES ACCELERATION DATA RECORDED UNDER TRAFFIC (TEST18) 34
FIGURE 3.10 PREDICTED MID-SPAN DISPLACEMENT IN VERTICAL AND TRAFFIC DIRECTION UNDER VERTICAL ACCELERATION RECORDED IN TEST 18 35
FIGURE 3.11 TIME SERIES ACCELERATION DATA RECORDED UNDER TRAFFIC (TEST1) 35
FIGURE 3.12 PREDICTED TRUSS MID-SPAN DISPLACEMENT IN VERTICAL AND TRAFFIC DIRECTION UNDER VERTICAL ACCELERATION RECORDED IN TEST 1 35
FIGURE 3.13 REVISED SIGN BRIDGE MODEL WITHOUT HORIZONTAL ARMS, LIGHTS AND WALKWAY 36
FIGURE 3.14 PREDICTED TRUSS MID-SPAN DISPLACEMENT IN VERTICAL AND TRAFFIC DIRECTION AFTER MODIFICATION UNDER VERTICAL ACCELERATION RECORDED IN TEST 18 36
FIGURE 3.15 PREDICTED TRUSS MID-SPAN DISPLACEMENT IN VERTICAL AND TRAFFIC DIRECTION AFTER MODIFICATION UNDER VERTICAL ACCELERATION RECORDED IN TEST 1 37
FIGURE 3.16 ABAQUS MODELS OF OSB-W 38
FIGURE 3.17 TIME SERIES ACCELERATION DATA RECORDED UNDER TRAFFIC 39
FIGURE 3.18 PREDICTED TRUSS MID-SPAN DISPLACEMENT IN VERTICAL AND TRAFFIC DIRECTION OSB-W 40
FIGURE 3.19 REVISED OSB-W MODEL WITHOUT HORIZONTAL ARMS, LIGHTS AND WALKWAY 40
FIGURE 3.20 PREDICTED TRUSS MID SPAN DISPLACEMENT IN VERTICAL AND TRAFFIC DIRECTION AFTER MODIFICATION OSB-W 41

List of Tables

TABLE 1.1 STRUCTURE GEOMETRY 3
TABLE 2.1 RAINFLOW DATA FIRST WEEK OSB-E 24
TABLE 2.2 RAINFLOW DATA SECOND WEEK OSB-E L FRAME BRACKET WELDS 25
TABLE 3.1 MATERIAL PROPERTIES 31
TABLE 3.2 COMPARISON OF THE NATURAL FREQUENCIES OF THE THREE MODELS 32
TABLE 3.3 NATURAL FREQUENCIES OF ORIGINAL OSB AND STRENGTHENED OSB 33
TABLE 3.4 COMPARISON OF RESPONSE MAGNITUDE OF ORIGINAL AND MODIFIED STRUCTURES TO RECORDED BASE ACCELERATIONS 37
TABLE 3.5 COMPARISON OF THE NATURAL FREQUENCIES OF THE TWO MODELS 39

Summary

This report documents a field and analytical study of the behavior of two overhead sign bridges to determine the cause of the vibrations observed. The sign bridges were mounted to prestressed concrete bridge girders at about the quarter point of the span. The responses of the sign bridges and the highway bridges were measured in the field to determine the amplitude and frequency of the vibrations as well as the cause of the vibrations. The sign bridges were excited by the vertical movement of the highway bridge from trucks traversing the bridge. The gust load from a truck passing under the overhead sign bridge was not the cause of the vibration.

Analytical studies of the sign bridges revealed that removal of the horizontal work platform, its railing, and the lights in front of the signs reduced the amplitude of vibrations in the sign bridge. The eccentricity of the load from these components caused a torsional rotation of the sign bridge during the passage of the trucks. Additionally, removal of the horizontal supporting arm eliminated the fatigue prone corner weld detail occurring at the joint of the horizontal support to the vertical sign support.

Fatigue stresses measured on the sign bridges revealed that except for the corner weld detail, the fatigue stresses in the sign bridge truss structure were too low to cause fatigue cracking in the truss and supporting structure members.

It is recommended that sign bridges not be mounted in the span of the highway bridge where ever possible. If they are mounted in the span of the bridge, the work platform, lights, and railing should not be installed since they greatly increase the amplitude of the sign bridge movement and are likely to fail in fatigue. The lights commonly used on these signs are no longer required with the new high reflective paints now available for signs.

Chapter 1

Introduction and Inspection of Sign Supports

The vibrations of two overhead sign bridges (OSBs) were measured and analyzed in this investigation. The investigation was prompted by motorists' and TxDOT personnel's visual observation of the OSBs vibrations. The structures are located on US290/SH71 in Austin, Texas. The sign bridges are steel truss structures attached to a prestressed concrete girder bridge. The OSBs are supported on slab extensions from the bridge deck rather than the pier caps. Traffic induced oscillations of the highway bridge are transmitted to the sign structure. Diaphragms between the girders underneath and adjacent to the OSB tower mounting points carry the tower loads into the superstructure.

The geometry of the structures is summarized in Table 1.1. The easternmost OSB investigated is labeled OSB-E and the westernmost OSB investigated is labeled OSB-W. Due to large movements of the sign, the sign and the mounting brackets were removed from OSB-W at the start of the study. The supporting brackets and sign were moved to the Ferguson Structural Engineering Laboratory to look for signs of fatigue distress and to measure geometry and weight. The geometry and weight were used to construct an analytical model. The results of the examination for fatigue distress are given at the end of this chapter.

Table 1.1 Structure Geometry

	OSB-E	**OSB-W**
Location	STA 10633+00	STA 10625+15
Highway Bridge Span	120'	110'
OSB Span	88'	72'
OSB Location (% of Span)	33%	23%
Signs	3	0
Girder Layout	Flared	Parallel

Figure 1.1 is a view, looking west, of both OSBs. The three signs on OSB-E are visible. OSB-W is between OSB-E and another more westerly OSB that has signs mounted. A walkway with a collapsed hand rail is cantilevered in front of the signs with lighting for the signs at the extremity of the cantilever structure. The sign and these ancillary components are attached to a steel wide flange section L frame which is bolted to the OSB.

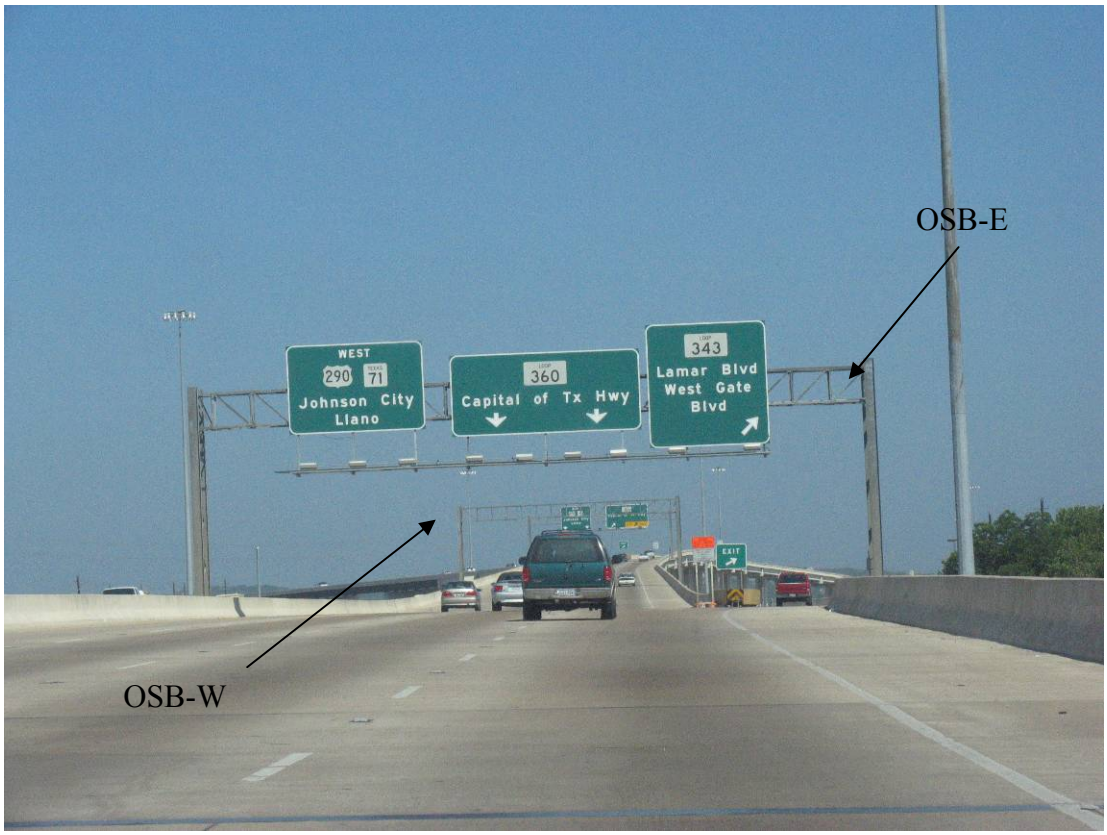

Figure 1.1 Overhead Sign Bridges Investigated

1.1 Overview of Field Studies

The vibrations of the two overhead sign structures were investigated. The results are summarized in Chapter 2. The investigation included 11 days of field measurements of the vibrations of the highway bridge spans and the two OSBs. Single and three axis accelerometers were used to measure the response of the structures to vehicle traffic. The high speed data acquisition system simultaneously recorded all channels which eliminated slewing of the data from one channel to another. The accelerations were measured at various locations on the OSB. The highway bridge response was measured at the base of the OSB. The measured acceleration records were used to determine the frequency response of the structures. The recorded acceleration was integrated twice with respect to time compute the displacements and mode shape of the structures.

The response of the OSB was also measured using a video system consisting of a video camera and a long focal length lens. The displacement of a unique target on the OSB was determined by tracking the target using specialized software.

The fatigue damage occurring in the sign was assessed by employing strain gages connected to a data acquisition system which processed and stored the data using a rainflow counting stress range collection scheme. Two weeks of strain gage data were recorded and analyzed.

1.2 Analytical Studies

Three dimensional models of the highway bridges and OSBs were developed. The models were used to determine the fundamental frequencies of the OSB and highway bridge structures individually and in a combined model which included both the OSB and the highway bridge. The individual OSB models were employed to evaluate the fatigue stresses in the structure by using the measured bridge accelerations as input to a dynamic analysis. The placement of strain gages on the structure was based upon the results of this analysis. The influence of the mass of the sign and the walkway in front of the sign on the OSB vibrations was determined using these models. The analytical results are given in Chapter 3.

1.3 Examination of Sign and Supports from OSB-W

The sign structure and its support from OSB-W were visually inspected at the laboratory. The individual pieces were weighed by recording the reading from a load cell connected to the overhead crane in the laboratory. The centers of gravity of the L frame support, sign, walkway and hand rail, and lights were estimated.

The critical location for fatigue cracking is the connection between the vertical and horizontal elements of the supporting L frame. Figure 1.2 shows the horizontal portion of the L frame with walkway and lights mounted. The vertical part of the L frame was cut off for shipping. A close-up of the welded connection is shown in Figure 1.3.

Figure 1.2 Horizontal Leg of L Frame

Figure 1.3 Critical Fatigue Detail

The ends of the stiffener fillet weld on both the vertical and horizontal leg are probable locations for fatigue cracking. These locations were visually examined. No fatigue cracks were found.

The mounting points between the L frame and the OSB showed signs of movement between the two structures. The galvanizing had worn away and corrosion staining was evident as shown in Figure 1.4. Considerable fretting has occurred at the connection point, which has removed the zinc coating from the support. The sign serves as a shear diaphragm between the L frames, causing them to resist the deformation of the OSB. Rust stains below the connection on other structures are as a visual indicator of OSB oscillations.

Figure 1.4 Fretting and Rust Staining on Vertical Supports

Chapter 2

Field Test Results

2.1 Overview of Field Tests

Field tests of the two sign bridges were conducted during the period from 7/28/05 to 12/13/05. The purpose of the field tests was to measure the response of the OSB-E and OSB-W to the highway bridge vibration and controlled pluck tests. The OSBs and/or bridge spans were instrumented with accelerometers, strain gages, and targets for the video displacement measurement system. The accelerometer data was used to determine the frequency response of the structures and the relationship between the bridge, OSB vibrations, and by double integration, to estimate the dynamic displacement of the structures under normal traffic conditions. The video displacement system was used to confirm the behavior measured by the accelerometers and to evaluate the ability of the technology to be used in a field environment. Strain gages were applied to OSB-E to measure the dynamically induced stresses in the sign bridges. The strains were measured during and after passage of a single truck followed by connection to a battery powered CR-23x data acquisition system which captured the strain data using a rainflow counting scheme. The rainflow counting was done over two 1-week periods. The rainflow counting technique is a means of counting the excursions in the measured strain signal to provide an estimate of the fatigue life of the structure. In addition to the tests performed under normal traffic, a pluck test was conducted at night with three of four lanes closed to traffic on each OSB to determine the natural frequencies of the structures.

2.2 OSB Natural Frequencies of Vibration—Pluck Test

A pluck test was performed on each OSB by suspending a weight from a cable attached at the midspan of the OSB truss. Releasing the weight causes a force impulse to excite the structure. The spectrum of the resulting acceleration data can be used to estimate of the natural frequencies of the OSB structure.

Figure 2.1 and Figure 2.2 show the pluck test data from each sign bridge. The upper plot in each figure is the time series data for the vertical and east-west components of the sign bridge accelerations. The east-west direction is parallel to the traffic direction of the roadway and transverse to the long axis of the OSB horizontal truss. The accelerations were measured at midspan of the sign bridges.

The spectra of the acceleration data were calculated using a fast Fourier transform (FFT), and indicate the strength of the acceleration signal at each frequency. The results of the frequency analysis are shown in the lower plot of each figure. For each OSB there is a dominant peak in the spectrum. This peak can be interpreted as the natural frequency corresponding to the mode of vibration most strongly excited by the pluck. The mode can be simply described as bending of the OSB truss at the center in the vertical

direction. The difference in the initial acceleration impulse in the two pluck tests is due to a difference in the weights attached and to a lesser extent the different in stiffness of the two sign bridges. OSB-E was loaded with 128 pounds, while OSB-W was loaded with 64 pounds.

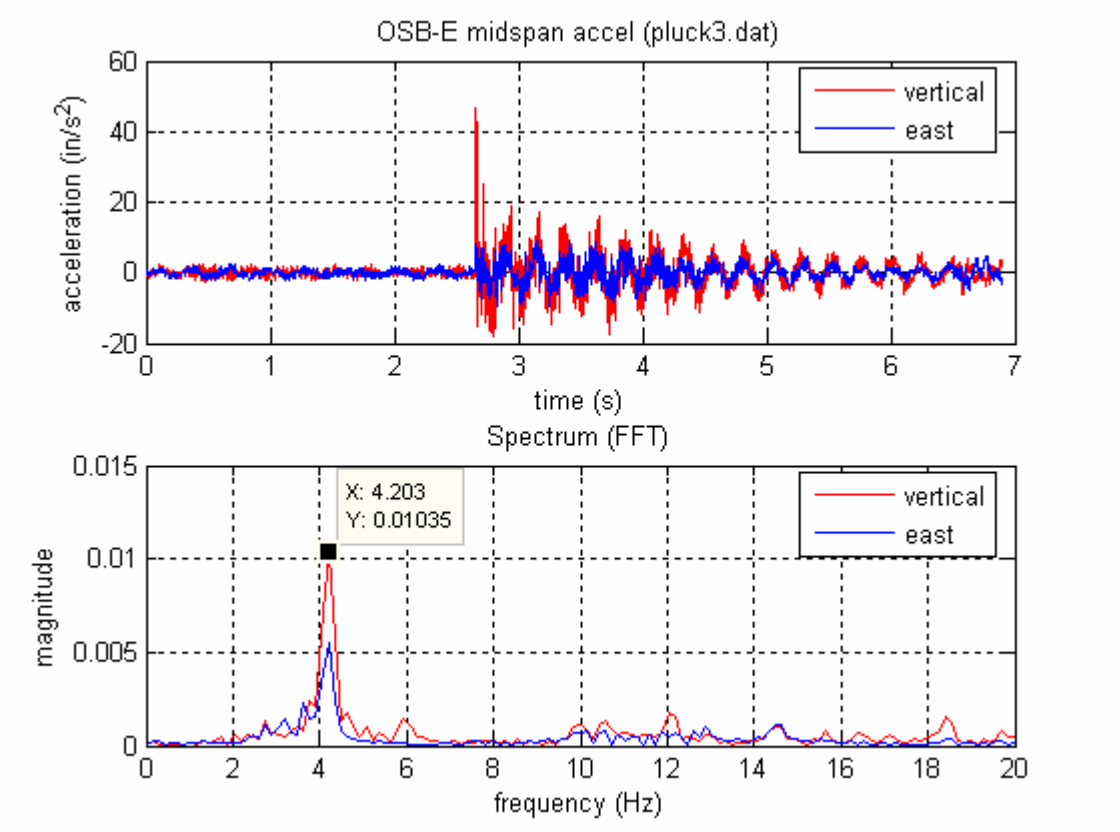

Figure 2.1 Pluck Test Results OSB-E

The spectra show a peak of approximately 4.2 Hz for OSB-E and 6.8 Hz of OSB-W. The difference in the natural frequency is consistent with the differences in geometric configuration and mass of the two structures. OSB-W is shorter in span and lighter due to the absence of signage, L-brackets, walkway, and lights. Since natural frequency of a simply supported beam vibrating in the fundamental flexural mode is a function of the reciprocals of length and mass, it follows that lower mass and less length result in higher natural frequency.

The damping factor of the OSB-E structure was estimated from the pluck test results. The lengthy duration of large motion events indicates low damping in the structure. This is reasonable considering that the only likely energy dissipation mechanisms are aerodynamic damping due to the signs and friction in the bolted connections.

The damping factor was estimated using a technique based on the logarithmic decrement method. That method was developed mathematically to analyze the free response of an impulse-excited (plucked) single degree of freedom (SDOF) system. In the SDOF case,

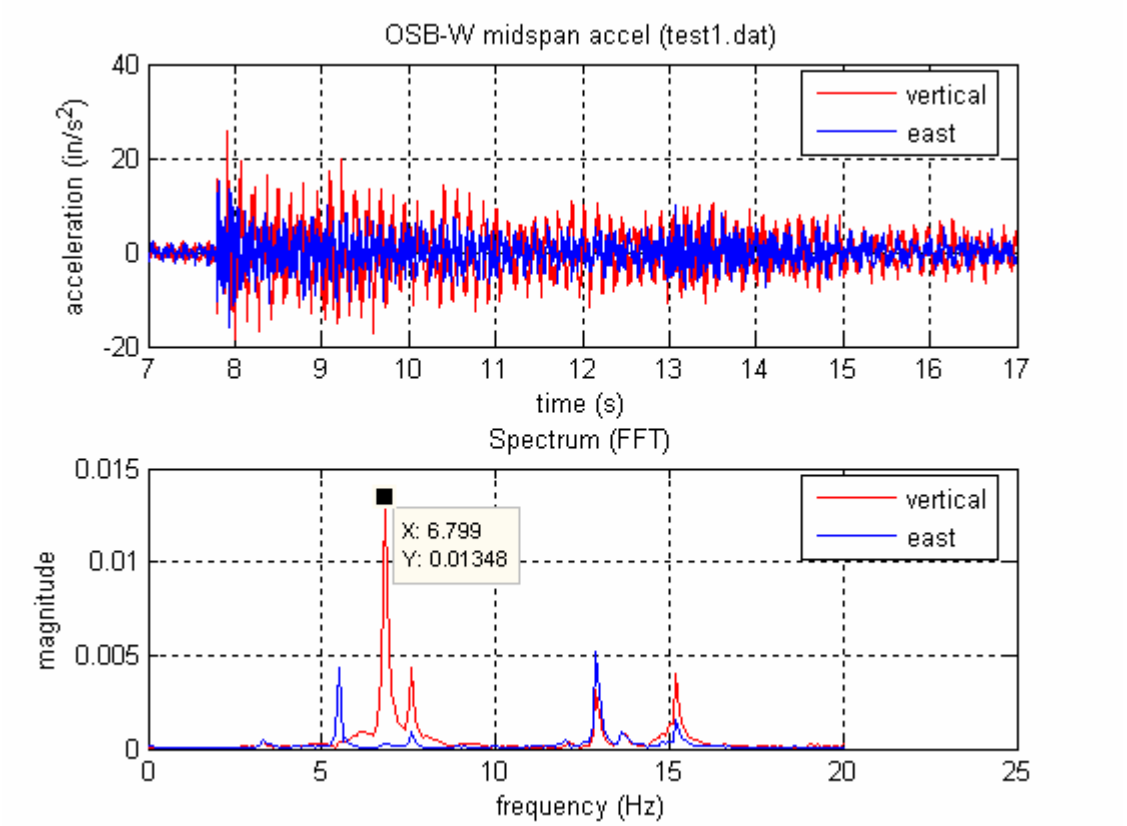

Figure 2.2 Pluck Test Results OSB-W

the free vibration is a decaying sinusoidal signal of a single frequency. The OSB structure, on the other hand, is a multi degree of freedom (MDOF) system whose response appears very noisy compared to the ideal case. The log decrement method was adapted to accommodate the experimental data. Software written to perform the analysis first takes the absolute value of the signal, so all peaks are positive. The peaks are identified based on the period of the fundamental frequency in the signal. These points were then plotted on a log scale and a best-fit line was computed. The damping factor was computed from the slope of the line. The pluck test data for OSB-E gives a damping factor of 1.8%, which is very low but typical of bare steel structures.

2.3 OSB Acceleration Data from Traffic Loads

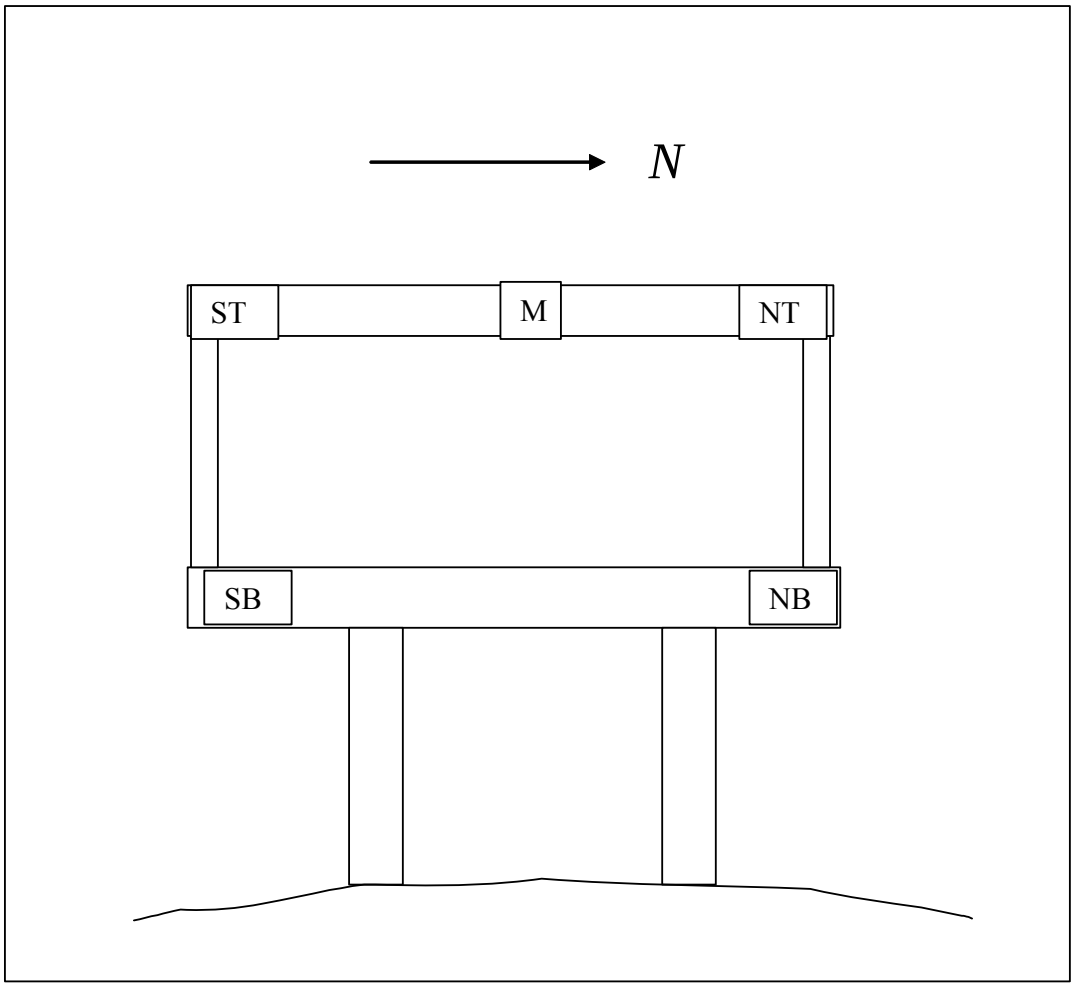

Figure 2.3 Location Instrumentation on OSB

Acceleration data was collected for both OSBs using accelerometers attached at the bases of the OSB columns, column tops, and truss midspan. At the column tops and truss midspan triaxial accelerometers were used, permitting collection of acceleration in three directions, x, y, and z. Accelerometers at column bases recorded vertical acceleration data only. Figure 2.3 shows the location of the accelerometers on the sign bridges and the label assigned to each location.

2.3.1 OSB-E Acceleration Data

Time series acceleration data was recorded under normal weekday traffic conditions. Figure 2.4 illustrates a typical event in which the motion of the bridge deck at the OSB-E location, measured at the north and south sides of the bridge, increases rapidly from a very quiet, low-motion state to vibrations in excess of 0.1 g. The spectral analysis of the data indicates that the dominant responses of the highway bridge are at frequencies above and below the frequency of 4.2 Hz excited in the pluck test. The measured acceleration was caused by the passage of a truck on the bridge. The measured bridge deck acceleration was as high as 0.2 g. Although the peak displacements of bridge deck are calculated to be no more than 0.1 inch, human observers standing on the bridge deck

perceived the high-motion episodes to be disturbingly strong as well as long-lasting (i.e., the vibrations do not damp out rapidly).

Large amplitude motion was observed visually on OSB-E. Movement is especially noticeable at the tips of the horizontal arms of the L-brackets supporting the lights and walkway. The acceleration measurements taken at the OSB horizontal truss had peaks as high as 360 in/sec^2 (0.94 g) at the top of the south column and 266 in/sec^2 (0.69 g) at the midspan of the OSB truss in the east-west motion of the OSB which is parallel to traffic direction.

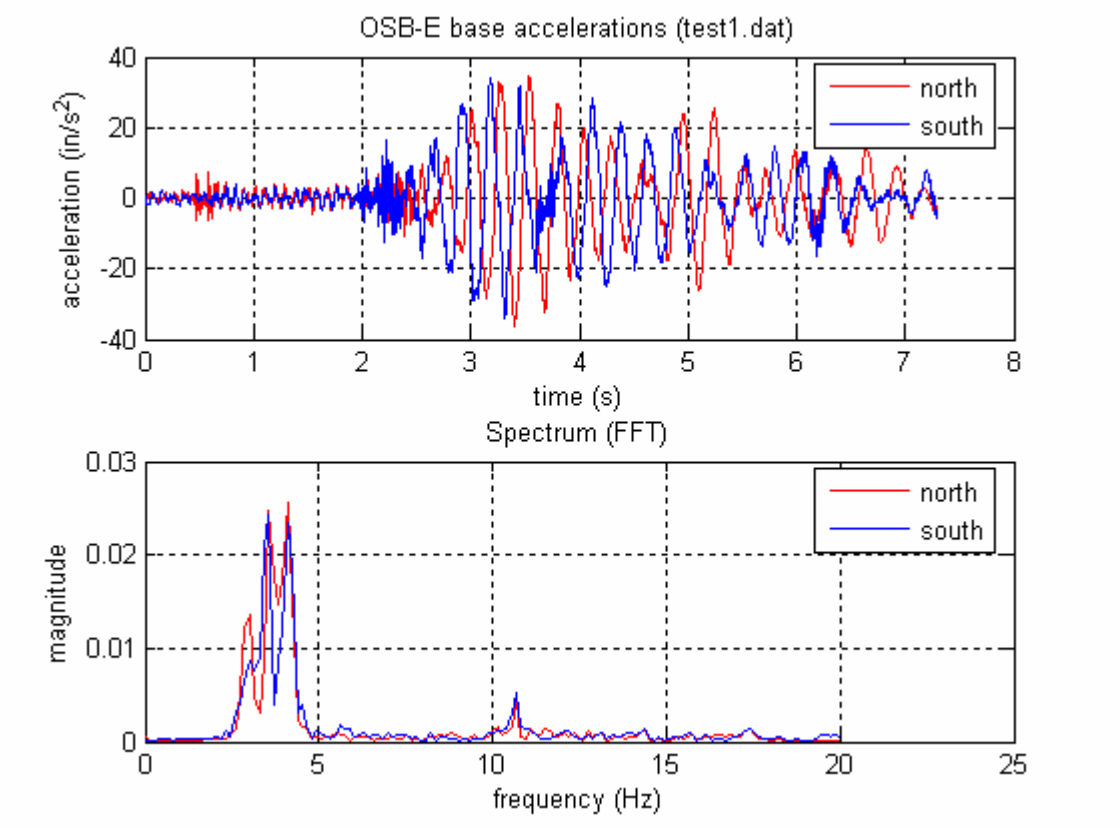

Figure 2.4 Horizontal Vibration of OSB-E

2.3.2 OSB-W Acceleration Data

OSB-W exhibited little observable motion under traffic. This can be attributed to the lack of attachments (i.e. signs and cantilever supports with the walkway and lights in front of the signs). The measured accelerations were also considerably lower than those of OSB-E with vertical midspan peak amplitude of 119 in/sec^2 (0.31 g) in the event shown in Figure 2.5. The large spectral peak near 7 Hz appearing in the vertical midspan motion signal is similar to the pluck test. Also noteworthy is the typically rapid onset of the oscillation after a period of low motion.

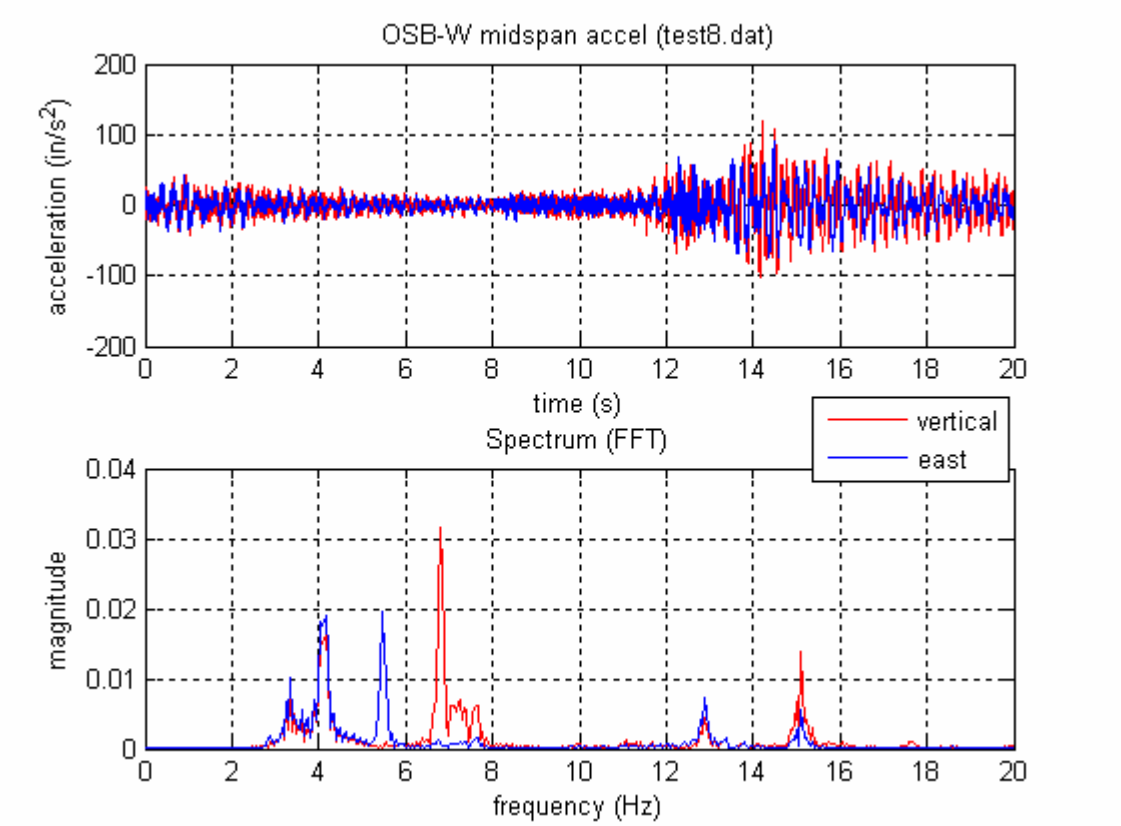

Figure 2.5 Oscillations of OSB-W

2.4 Highway Bridge Mode Shapes

A vibrating structure with multiple degrees of freedom can assume multiple mode shapes in free vibration depending on the excitation. A single span of the US 290 / SH 71 (a.k.a. Ben White) highway bridge can be thought of as a simply-supported, wide, shallow beam or a ribbed plate supported at two edges. A three-dimensional finite element model was used to calculate the dynamic behavior of the bridge and sign structure. The results of the dynamic analysis are presented in Chapter 3. A simplified model with two modes of vibration, flexural and torsional, was used to analyze the field data.

In a simplified model, the highway bridge span can bend like a simply-supported beam due to point and distributed loads. It can also twist about its long axis (axis parallel to traffic direction), so the north rail is higher or lower than the south rail. Figure 2.6 shows highway bridge deck displacements at the OSB-E location computed from the acceleration data. The fact that the motions of the north and south edges of the bridge deck are out of phase indicates that the vibration is not in a pure beam-bending mode from support to support. In Figure 2.7 the same data is decomposed into a bending component and a rotation component by averaging and differencing the data, respectively. In the computation, y1 and y2 are the north and south edge vertical displacements, respectively. The result shows that the rotation, or twisting, component is much higher than the bending component, especially at the onset of the vibration.

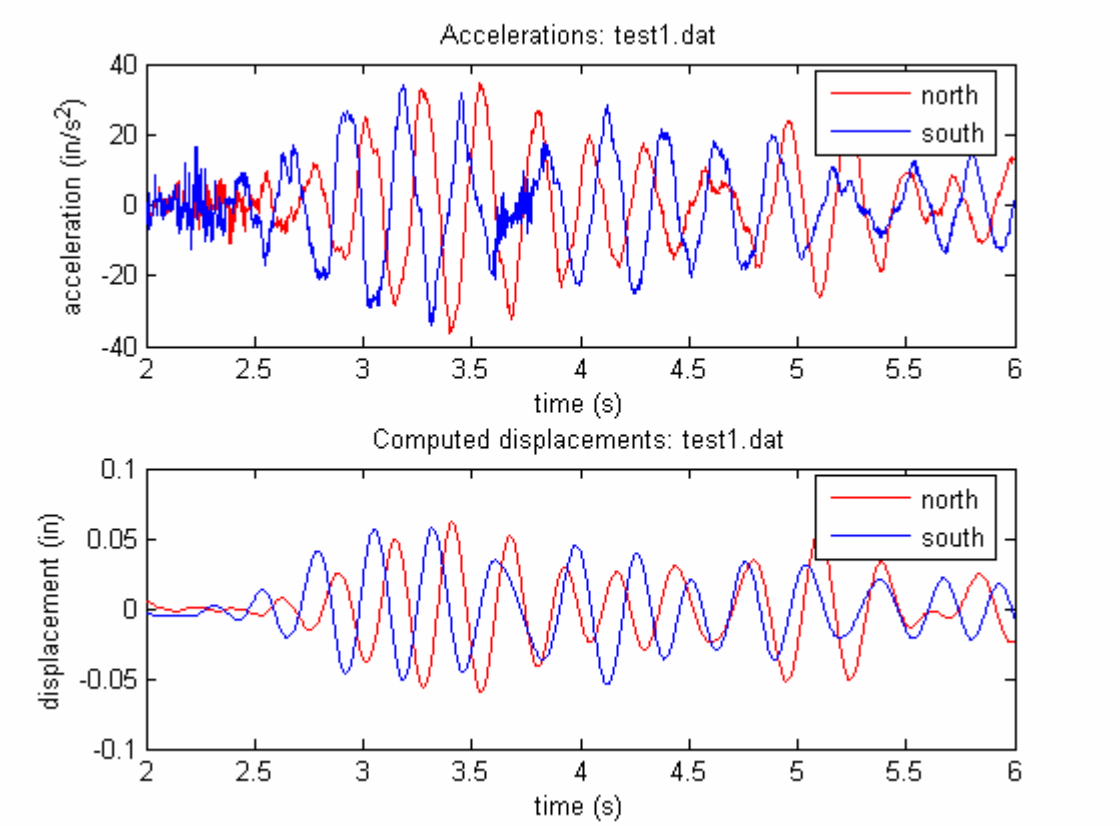

Figure 2.6 Accelerations and Displacements of Bridge Deck at OSB-E

Examination of Figure 2.6 reveals that the initial excitation is stronger at the south edge than at the north. The first second of the data shows the amplitude of the south edge vibration builds up faster than the north edge. This suggests that a heavy truck traveling in the south (left) lane crossed the bridge at this time. Visual observations of traffic and bridge motion indicate that truck loads in the left and right lanes of the four traffic lanes can cause large motions in both the highway bridge and the OSB. The torsional mode did not always predominate. Figure 2.7 shows a case where the bending mode of vibration is greater than the rotational, or torsional, mode.

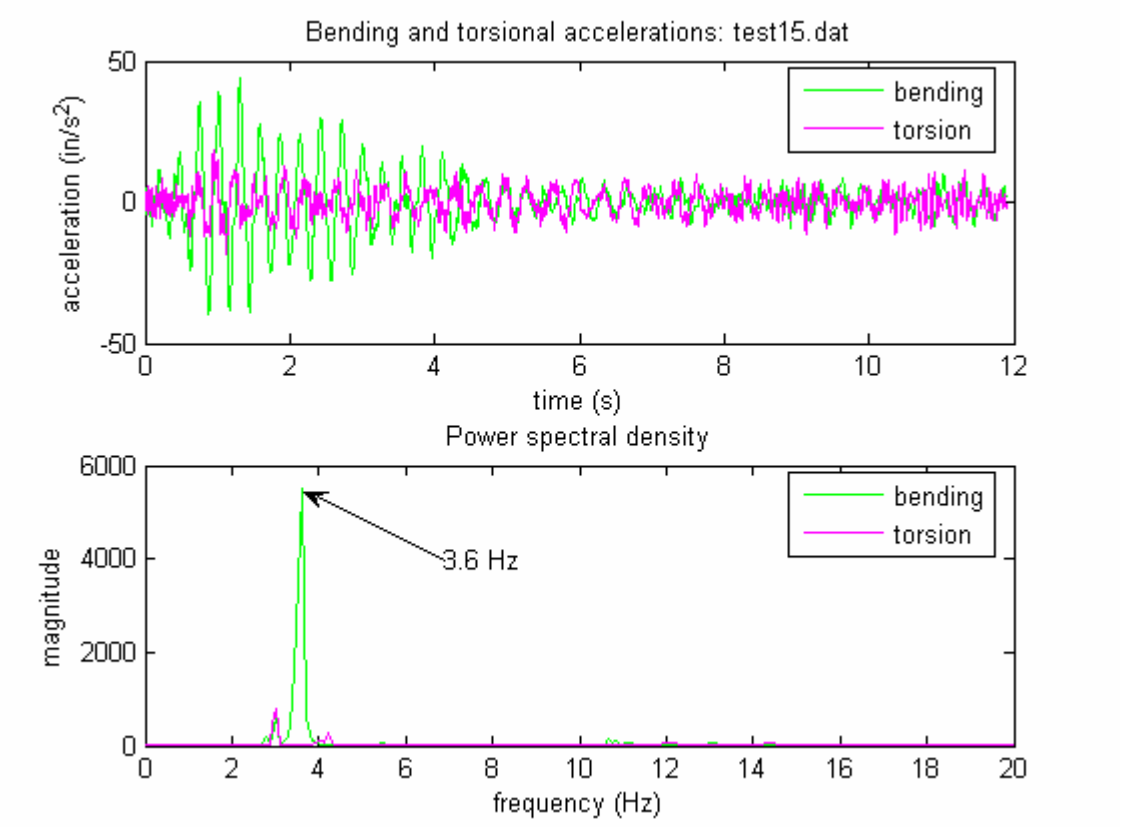

Figure 2.7 Bending and Torsional Oscillations of OSB-E

2.5 Highway Bridge and OSB Vibration Analysis

The field measurements and human observations support the conclusion that OSB motion is caused by vibrations of the supports on the highway bridge due to the passage of a truck. The relationship between the frequency of the bridge vibration and the OSB vibration was examined to determine the relationship between the frequency of the highway bridge and the OSB. This is important because if the resonances coincide in frequency, the OSB will be excited at or near its resonance, and the response will be greatly amplified. In a theoretical undamped structure, a finite excitation at the resonant frequency causes a response of infinite amplitude. The practical application of this information is to permit "tuning" of the OSB resonances, by design or retrofit, so they do not correspond to the dominant excitation frequencies.

For OSB-E, the vertical accelerations of the bridge deck typically exhibit three strong spectral peaks at 3.0, 3.6, and 4.1 Hz as shown in Figure 2.8. Figure 2.9 shows two strong spectral peaks in the vertical accelerations of the deck of the OSB-W highway bridge in the same frequency range. Although there are differences between the two bridge spans, the similarity of geometries and the similarity of the 3 to 4 Hz range of the spectra suggest that these frequencies are the resonances of the highway bridge.

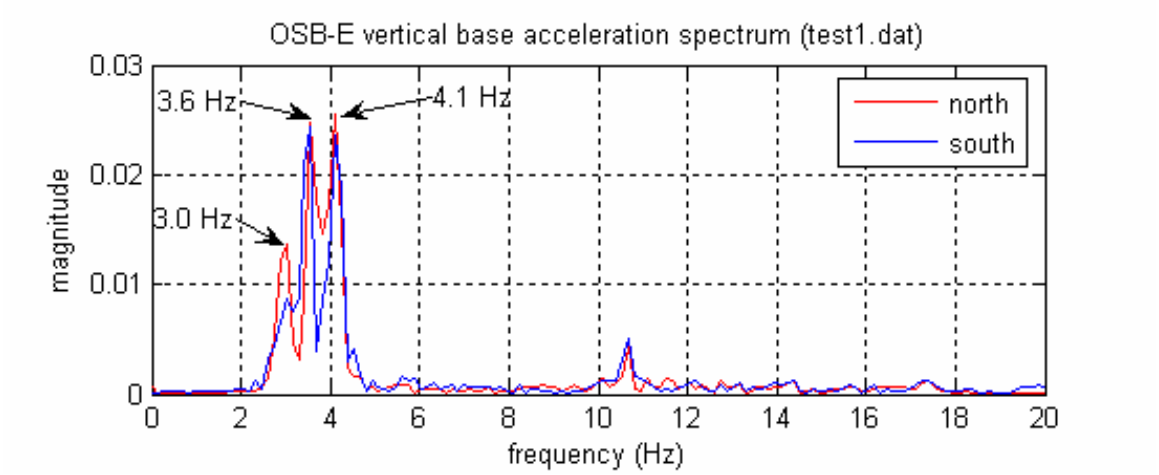

Figure 2.8 Highway Bridge Deck Acceleration Spectrum at OSB-E

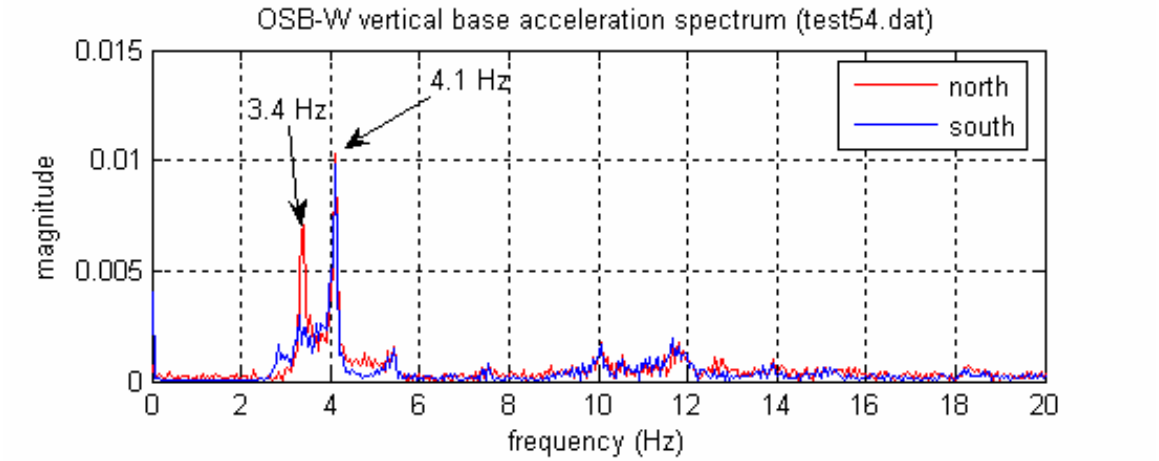

Figure 2.9 Highway Bridge Deck Acceleration Spectrum at OSB-W

The pluck tests conducted on the two OSBs resulted in markedly different responses. Referring again to Figure 2.1 and Figure 2.2, the OSB-E pluck spectrum is dominated by a 4.2 Hz peak, while the main frequency of the OSB-W pluck is around 6.8 Hz. As discussed earlier, the difference in these responses agrees well with the differences in mass and stiffness between the two OSBs. Another key observation is that the OSB-E vertical midspan response is near the range of the main highway bridge excitation, while the OSB-W response is considerably higher than the highway bridge. The closeness of the highway bridge and OSB response frequencies for the east bridge agrees with the observation that large motion occurs frequently in OSB-E while little motion was evident in OSB-W and supports the notion that the closeness of the natural frequencies of the highway bridge span and the OSB is amplifying the response of the sign bridge.

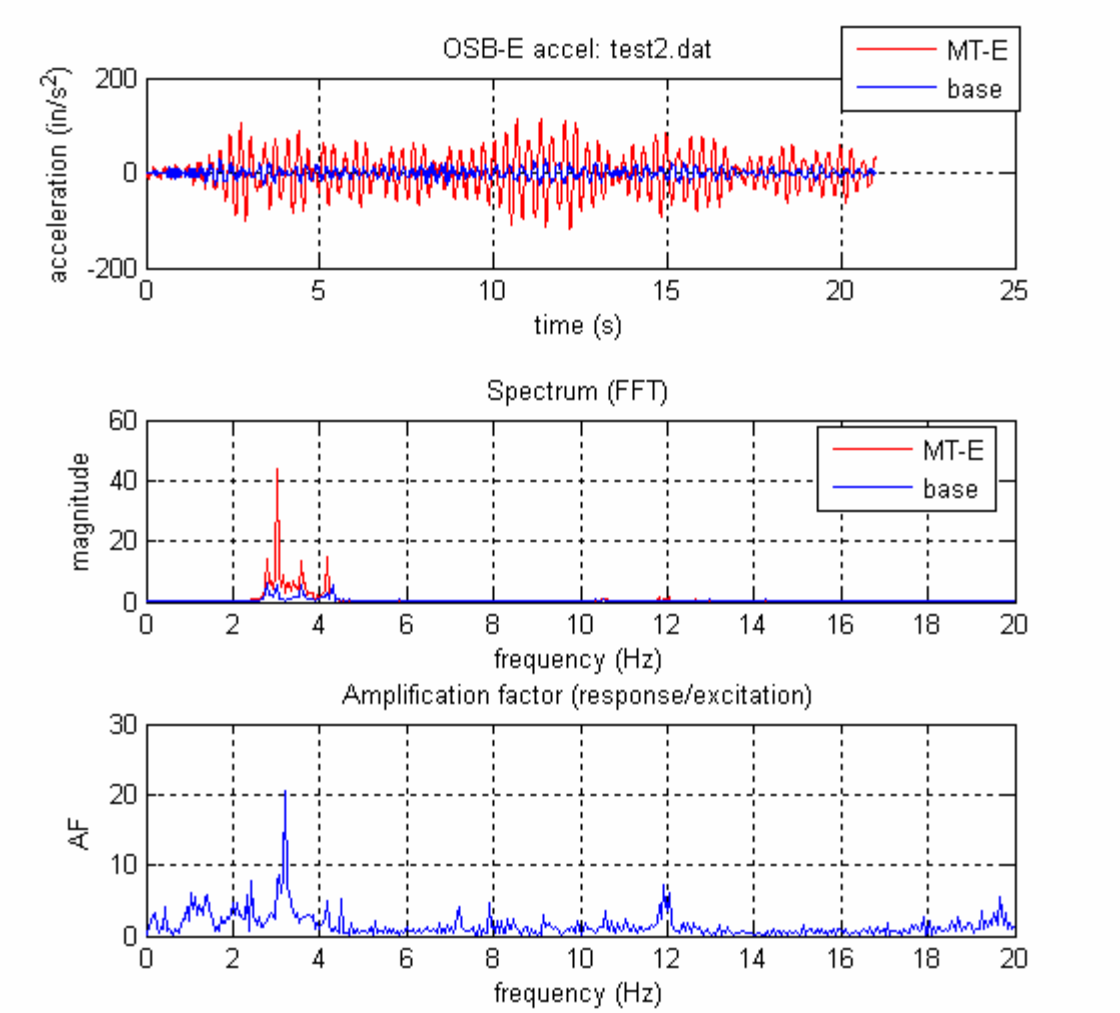

Figure 2.10 Horizontal Response of OSB-E to Vertical Bridge Vibration

The relationship of the excitation and response can be studied by computing the amplication factor (AF). The AF has been computed by summing the spectra of the north and south vertical bridge deck accelerations (labeled as base in the figures) as a measure of the excitation input into the OSB. The OSB response was taken as any of the acceleration signals measured at the column tops or truss midspan. The AF is simply the ratio of the response signal strength to the excitation at any given frequency. The response consists of both forced vibration (due to excitation) and free vibration. The AF plot tends to highlight the OSB resonances (free response) and diminish the forced response frequencies.

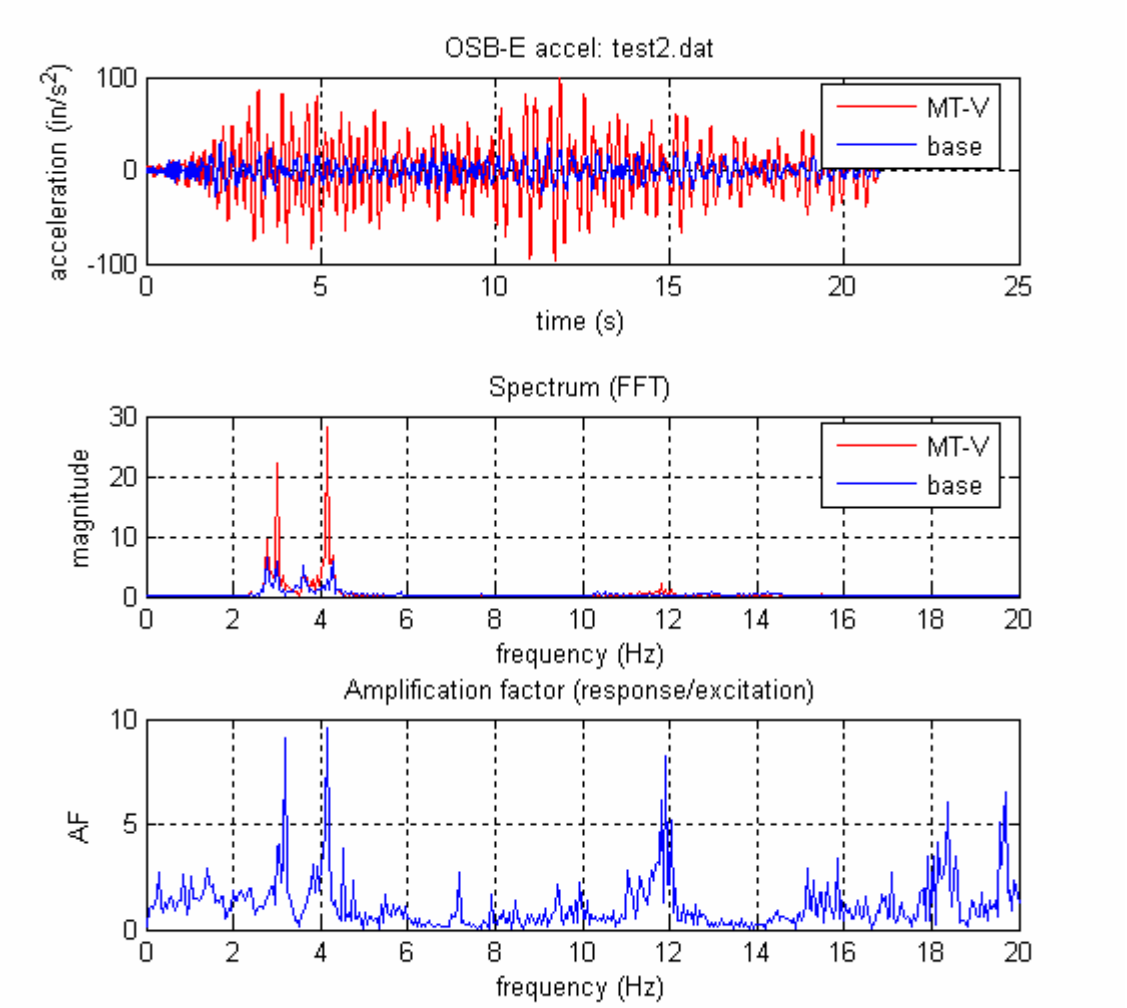

Figure 2.11 Vertical Response of OSB-E to Vertical Bridge Vibration

The amplification plots for OSB-E for the midspan horizontal and vertical accelerations are plotted in Figure 2.10 and Figure 2.11 respectively. The 4.2 Hz natural vertical frequency of the OSB-E is clearly shown in Figure 2.11 along with a peak near 3 Hz and some higher frequency components that appear negligible in the spectrum (they could be harmonics). The peak at 3 Hz is also evident in the horizontal response shown in Figure 2.10 but the peak at 4.2 Hz is missing. The 4.2 Hz response is a torsional response of the OSB which produces a horizontal as well as a vertical displacement of the top chord of the OSB.

The AF plot for the OSB-W vertical midspan acceleration in Figure 2.12 shows a very distinct AF peak at the 6.8 Hz OSB resonance. The spectral peaks in the 4 to 6 Hz range of the highway bridge (base) do not produce a significant response from the OSB. They do not produce a significant AF plot, showing that the response of the OSB is simply the forced response of the OSB to the bridge without significant amplification. Even though the OSB and highway bridge frequencies do not coincide in the west bridge, significant

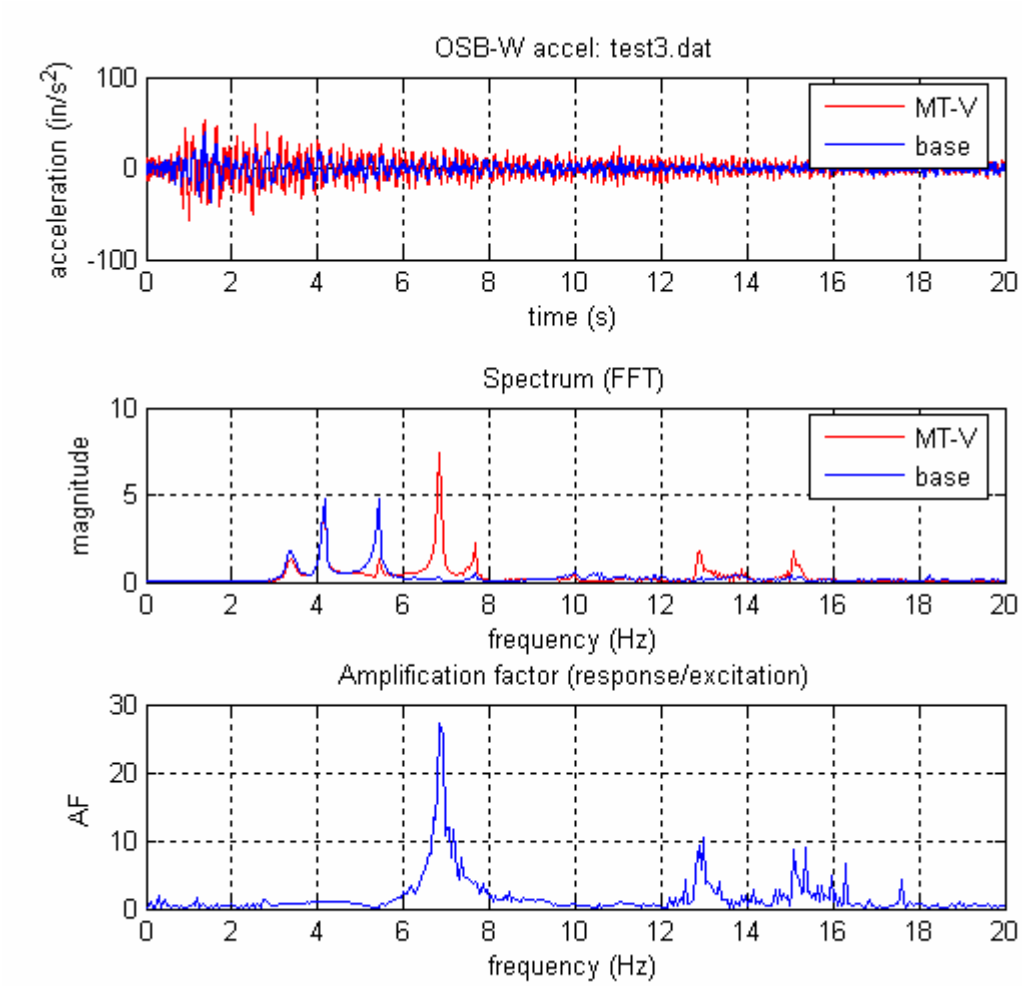

Figure 2.12 Vertical Response of OSB-W to Vertical Bridge Vibration

movement of the sign bridge occurred. The accelerations measured at midspan of the sign bridge were significantly larger then those measured at the base of the sign.

2.6 Displacement Measurements Using Video Images

At the outset of this project, it was observed that the capability of making displacement measurements of the structure through remote, non-contact means would be valuable. Such a capability would reduce cost, labor, and safety risks from lane closures and installation of equipment on the structure and also eliminate the need to integrate the acceleration data twice to calculate the displacements. A small study was undertaken to capture video imagery of the OSB-E in motion and extract dynamic displacement data using image analysis software. The displacements from the video measurements were compared with those estimated from the acceleration data.

2.6.1 Video Measurement Method

Video displacement measurements were made using a video camera with a telescopic lens mounted on a tripod. The camera was located at ground level one block north of the OSB-E location. The camera was zoomed in a selected feature of the OSB structure, or a video target attached to the structure, and the video imagery was recorded on a VCR.

In the laboratory, the video data was digitized and analyzed using pattern recognition and target tracking software developed by researchers at Ferguson Lab. A distinct feature in the video image is selected as a target. Using knowledge of the actual dimensions of the target feature, the distances in the image are calibrated in units of pixels per inch (a pixel is a "picture element", that is, one dot in the digitized image).

The video sequence is then analyzed frame-by-frame. In each frame, target tracking software searches for the target pattern. When it is found, the target's location in the frame is computed to an accuracy of one-half pixel. The motion of the target can then be computed as relative displacement in inches from one frame to the next in two dimensions, vertical and horizontal. Given the standard frame rate of 30 frames per second, the time increment between data points is 33 milliseconds. In this way, a complete time series data set can be constructed with vertical and horizontal components at a 30 Hz sample rate.

2.6.2 Video Data Results

Figure 2.13 is a comparison of displacement data extracted from the video imagery with displacements computed from the acceleration data. Synchronization of the two data sources was challenging, but the analysts were able to identify a given motion event in both data sets. The plots of displacements from the two sources show a typical high amplitude motion event caused by the passage of a heavy truck.

In order to analytically demonstrate the correspondence between the two plots, the cross correlation function was computed for the 10 seconds of video-source data at varying time offsets within the accelerometer-source data. The peak in the correlation plot at 4.8 seconds indicates that there is a 4.8 second time shift between the two signals which was calculated assuming the beginning of each signal is at time = 0.

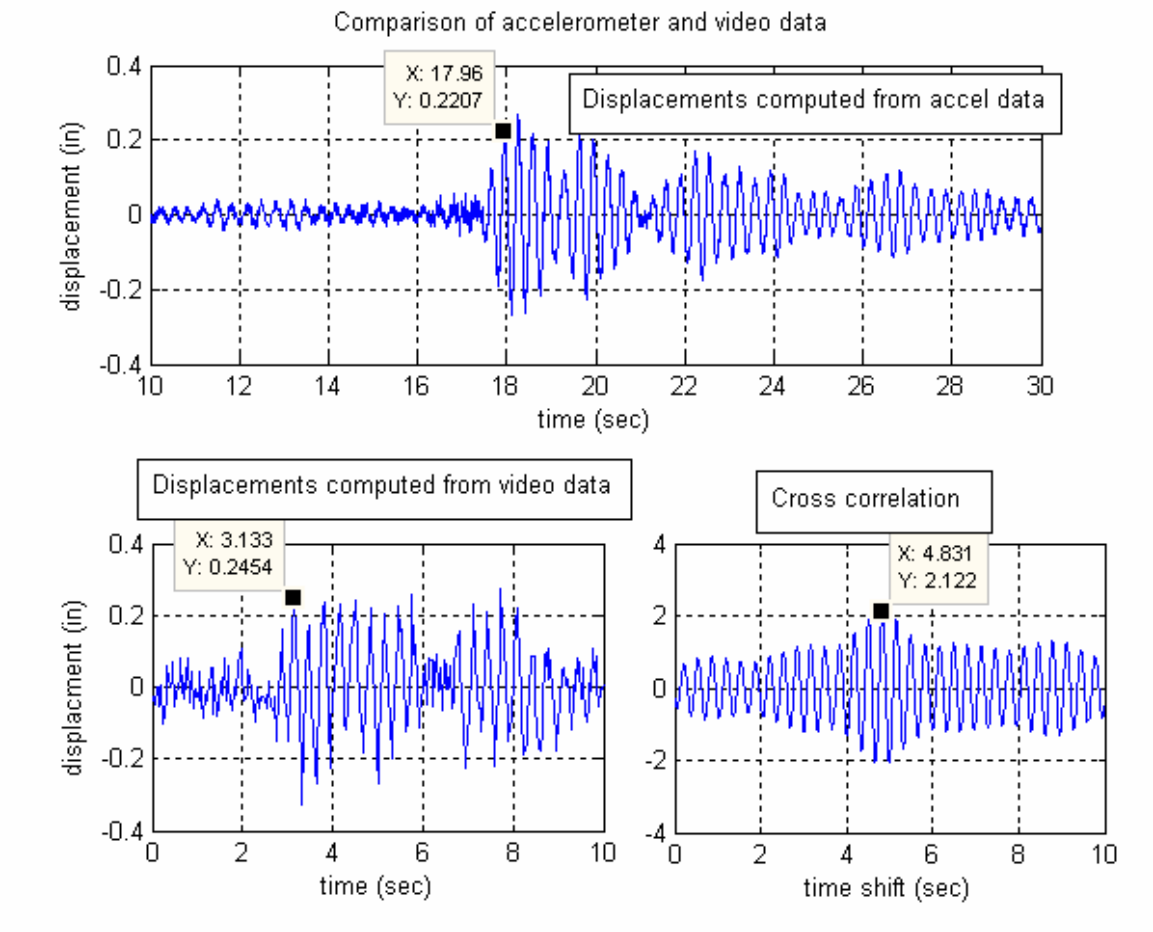

Figure 2.13 Comparison of Displacement from Video and Acceleration Data OSB-E

The two points marked in the displacement plots are 14.8 seconds apart. However, the accelerometer-sourced data begins at time = 10 seconds. The time shift is actually 4.8 seconds as shown in the cross-correlation. Visually the two signals are very similar in form and the amplitudes agree well. Likewise, frequency analysis (FFT) of the video-source displacement data gives very good spectral results compared to the acceleration data.

A number of improvements to the video measurement technique are possible. First, a camera with higher resolution and higher frame rate would increase the accuracy of the measurements in both time and distance. Improved optical components would permit higher magnification of the image as it is recorded. Additional attention must be paid to the camera mounting arrangement to ensure minimum vibration of the camera.

Overall, the video displacement measurement technology has proved to be a very promising technique for performing remote non-contact measurements. The technique offers significant potential savings in cost and labor in performing this type of structural

dynamics study and produces results comparable to those obtained with other instruments.

2.7 OSB-E Stain Gage Data and Fatigue Life Estimate

Strain gages were installed at seven locations on OSB-E. The locations were selected using the results of finite element analysis of the OSB excited by the measured highway bridge accelerations as input to the model. Locations near critical details that had high stress ranges were selected. These included the connections at the knees of three of the L-brackets supporting the signs, walkway, and lights, the two chords of the OSB truss where the L-brackets are connected, one angle at the top of the north column which connects the truss chord to column, and one on the north column W-section near the baseplate weld.

2.7.1 OSB-E Strain Time-Series Data

Time series strain data were captured under normal weekday traffic loads. The strain data were used to compute stress ranges, which agreed well with the FEA analysis results. The spectra of the strain signals corresponded well with the acceleration data, as expected.

2.7.2 OSB-E Long Term Rainflow Analysis

The strain gages were monitored for two one-week periods using a Campbell Scientific data logger programmed to execute a standard rainflow counting algorithm. The rainflow analysis accumulates the number of cycles that occur at given stress ranges. The resulting data is then used to estimate the rate at which fatigue damage is occurring in different OSB connections.

Using the fatigue design equations given in the AASHTO LRFD Bridge Design Specification, the fatigue life was computed at each location for each category in the specification. If the measured maximum stress range was less than the threshold value for the fatigue category, the fatigue life shown in the tables is given as infinite. If the maximum stress range exceeded the threshold the fatigue life in years was calculated as:

$$\text{Fatigue life in years} = \frac{\text{Fatigue life of detail}}{(\text{cycles per week}) \times 52.14} = \frac{\dfrac{A}{S_{re}^3}}{(\text{cycles per week}) \times 52.14}$$

The values of A are tabulated in the AASHTO Specifications. The cycles per week are listed in the table for each detail and recording period. The effective stress range was calculated using Miner's linear cumulative damage hypothesis as:

$$S_{re} = \left(\sum S_{ri}^3 \gamma_i\right)^{\frac{1}{3}}$$

Where γ_i= number cycles at stress range S_{ri} divided by total number of cycles.

Tables 2.1 and 2.2 show the resulting fatigue life estimates for each of the one-week data sets collected. The data from the first week showed that the stress ranges in sign bridge truss chords, locations MN and MS in Table 2.1, which are bolted angle members, have measured stress ranges far below the fatigue threshold for a category D the lowest fatigue category for a mechanically fastened structure. The stress ranges at the weld members at the top of the support structures and at the base, locations NT and NB, are also very small. Their fatigue life using the lowest fatigue category, category E', is over 100 years. The area of concern is the welded connections at the knees of the L-brackets, LM in Table 2.1, which support the walkway and lights in front of the sign. The stress ranges for the middle support instrumented was less than 10 years for a category E detail. The stiffened weld detail connecting the vertical and horizontal legs of the support is shown in Figure 2.14. This detail does not fit the fatigue categories in the AASHTO specification. It is estimated to produce a fatigue resistance less than or equal to a category D and better than a category E' detail.

The second week of data collection concentrated on gathering more data on these support bracket welds. Two additional brackets were instrumented the north end support, LN, and the other at the south end support, LS. The results from this second week of data are listed in Table 2.2. The results for the center support LM was the almost identical to the results of the previous week test. The effective stress ranges where nearly identical and the number of cycles recorded for the two tests was also very similar. The other two brackets had slightly smaller recorded stress ranges and number of cycles. The results indicate that these welds are likely to fail in fatigue if left in service.

Table 2.1 Rainflow Data First Week OSB-E

	Location	NT	MN	MS	LM	NB
	S_r max (ksi)	4.1	4.6	3.5	13.9	3.5
	S_{re} (ksi)	1.11	1.15	1.00	2.19	1.04
	Cycles/week	53,749	103,552	69,897	291,064	42,399
	Cycles/year	2,802,626	5,399,497	3,644,629	15,176,909	2,210,805
Fatigue Category	S_r threshold (ksi)	Fatigue Life Years				
A	24	Infinite	Infinite	Infinite	Infinite	Infinite
B	16	Infinite	Infinite	Infinite	Infinite	Infinite
B'	12	Infinite	Infinite	Infinite	38	Infinite
C	10	Infinite	Infinite	Infinite	28	Infinite
C'	12	Infinite	Infinite	Infinite	28	Infinite
D	7	Infinite	Infinite	Infinite	14	Infinite
E	4.5	Infinite	134	Infinite	7	Infinite
E'	2.6	102	47	107	2	157

Table 2.2 Rainflow Data Second Week OSB-E L Frame Bracket Welds

Location		LN	LM	LS
S_r max (ksi)		10.2	11.3	9.6
S_{re} (ksi)		1.98	2.20	1.86
Cycles/week		190,797	234,891	176,011
Cycles/year		9,948,701	12,247,888	9,177,716
Fatigue Category	S_r threshold (ksi)	Fatigue Life Years		
A	24	Infinite	Infinite	Infinite
B	16	Infinite	Infinite	Infinite
B’	12	Infinite	Infinite	Infinite
C	10	57	34	Infinite
C’	12	Infinite	Infinite	Infinite
D	7	28	17	37
E	4.5	14	8	19
E’	2.6	5	3	7

Figure 2.14 Support Bracket Weld Detail

Chapter 3

Analytical Investigation of the Vibrations on Overhead Sign Bridge

A finite element model of the sign and highway bridges was developed for each sign bridge location. The general purpose finite element program ABAQUS was used for the analysis. The analysis was performed to evaluate the dynamic behavior of the sign and highway bridges alone, the sign and highway bridges together as a system, the fatigue stresses in the sign bridges, and the influence of changes to the sign bridges upon their expected dynamic response.

3.1 Geometry of Overhead Sign Bridges

The shop drawings of both overhead sign bridges were not available. The geometry information needed for finite element modeling was obtained from Texas DOT standard design plans and measurement of walkways and sign removed from OSB-W and measurements at the site. A portion of the standard bridge plan sheet is shown in Figure 3.1. The details of each sign bridge model are given in the next sections.

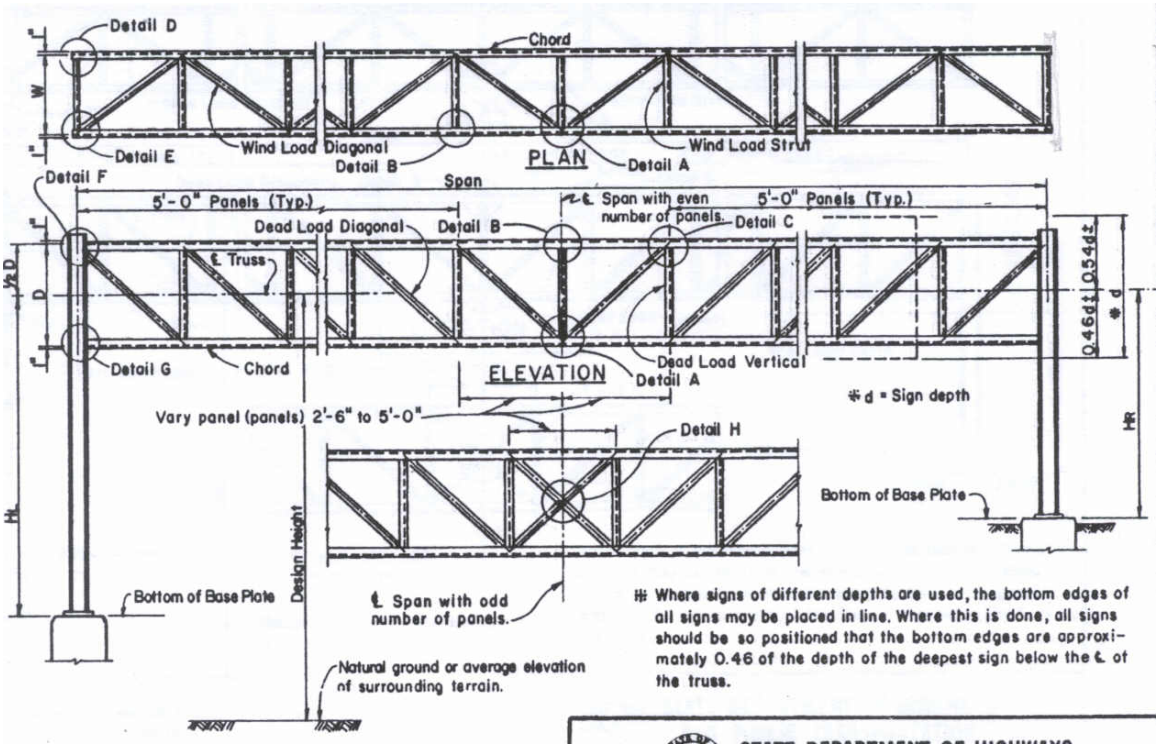

Figure 3.1 Standard Design of Overhead Sign Bridge

3.1.1 Detailed Geometry of OSB-E at Station 10633+00

A listing of the geometry of the East sign bridge is given below along with a schematic drawing of the geometry used in the analysis.

Columns:

- Left column height: 26.42 ft
- Right column height: 24.50 ft
- Column spacing: 6.5 ft
- Column: W16×36
- Bracing: 2 L_s 3×2.5×1/4”
- Truss bearing angle: L5×5×3/8”

Truss:

- Real Span: 87.333 ft (Design span: 90 ft)
- Height: 4.5 ft
- Width: 4.5 ft
- Chord: L 3.5×3.5×3/8” (HS50)
- Dead load diagonal: L2.5×2.5×3/16”
- Wind load diagonal: L3×3×1/4”
- Dead load vertical: L3×2×3/16”
- Wind load strut: L2×2×3/16”

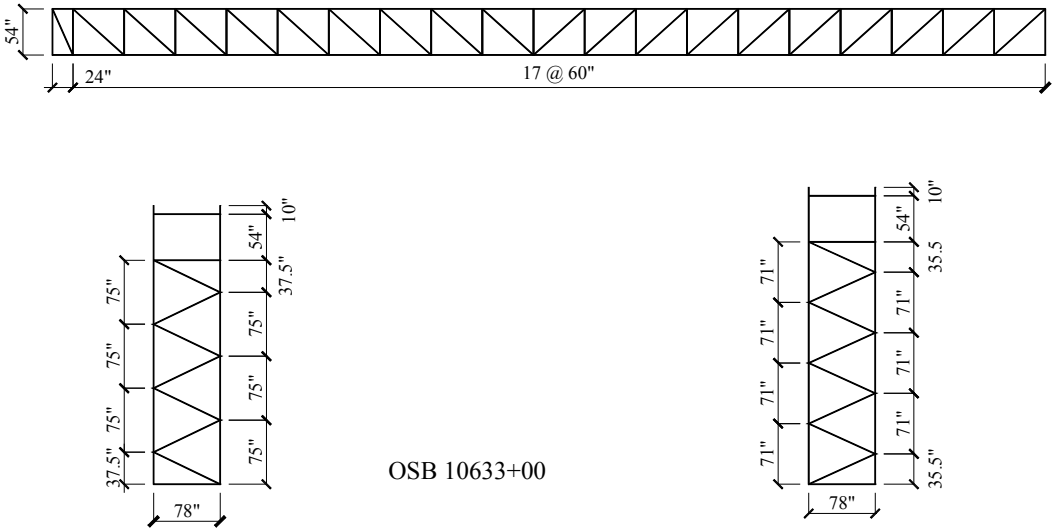

Figure 3.2 Schematic of OSB-E Structural Model

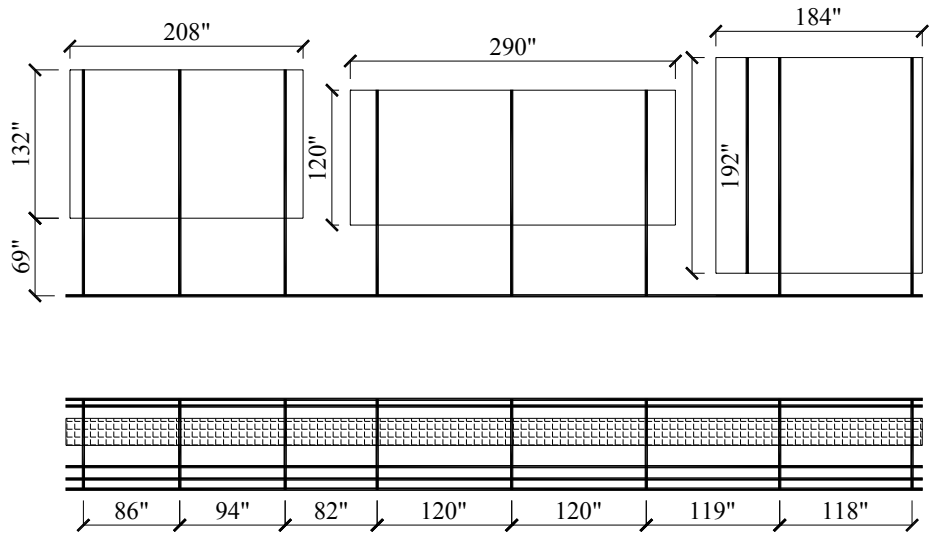

Figure 3.3 Sign and Sign Support Layout OSB-E

Sign frames and panels:

Frame: S4×7.7
Light mounting channel: A=0.51 in^2, 1.73 lb/ft
Light and conduit: 28 lb each
Cat walk: steel channel, 24 in by 3 in, 12.72 lb/ft
Railing: 7.55 lb/ft

3.1.2 Detailed Geometry of OSB-W at Station 10625+15

A listing of the geometry of the West sign bridge is given below along with a schematic drawing of the geometry used in the analysis.

Columns:

Left column height: 26.08 ft
Right column height: 24.50 ft
Column spacing: 6.5 ft
Column: W16×36
Bracing: 2 L_s 3×2.5×1/4”
Truss bearing angle: L5×5×3/8”

Truss:

Real Span: 73.500 ft (Design span: 75 ft)
Height: 4.5 ft
Width: 4.5 ft

Chord: L 3.5×3.5×5/16” (HS50)
Dead load diagonal: L2.5×2.5×3/16”
Wind load diagonal: L3×3×3/16”
Dead load vertical: L2.5××3/16”
Wind load strut: L2×2×3/16”

Sign frames and panels:

Frame: S4×7.7
Light mounting channel: A=0.51 in^2, 1.73 lb/ft
Light and conduit: 28 lb each
Cat walk: steel channel, 24 in by 3 in, 12.72 lb/ft
Railing: 7.55 lb/ft

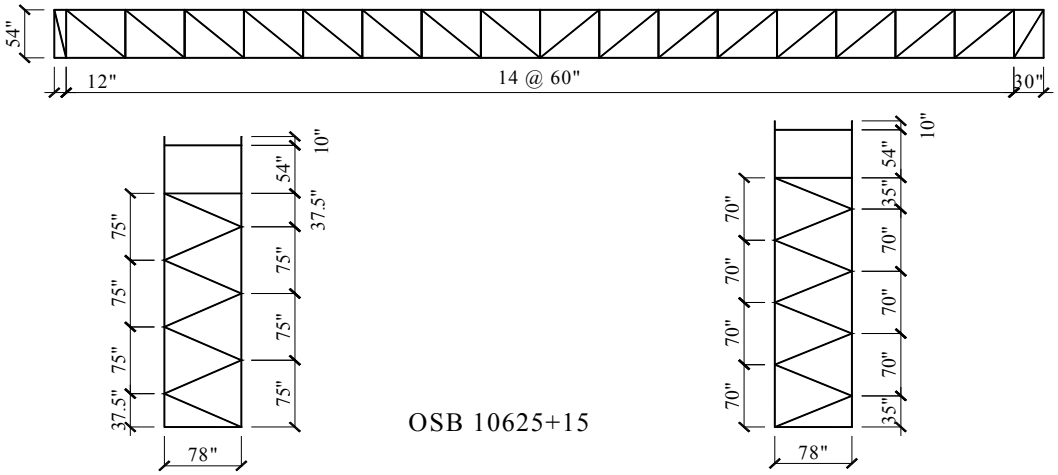

Figure 3.4 Schematic of OSB-W Structural Model

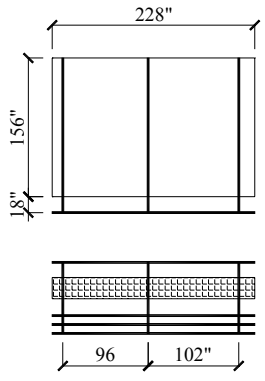

OSB 10625+15 SIGN FRAMES AND PANELS

Figure 3.5 Sign and Sign Support Layout OSB-W

3.1.3 Material Properties

All of the analyses were performed assuming elastic behavior. The model of the highway bridge assumed the sections were uncracked. The elastic properties input into the models are given in the table below. The concrete values were based upon the design strength of the girders.

Table 3.1 Material Properties

Material	Young's Modulus, ksi	Poisson's Ratio	Density, lb/in^3
Steel	29,000	0.28	0.2836
Aluminum	10,410	0.33	0.0978
Concrete	5,000	0.20	0.0831

3.2 Analysis of OSB-E

3.2.1 Natural Frequency Analysis

The three finite element models generated are shown in Figure 3.6. They consisted of models of the sign bridges and highway bridges alone and combined models which incorporated both structures for each sign bridge location. A modal analysis was performed on each model to determine their fundamental frequencies of vibration. The results at given in Table 3.2 and the mode shapes are shown in Appendix A. The results in Table 3.2 are ordered in terms of increasing frequency and similar mode shapes.

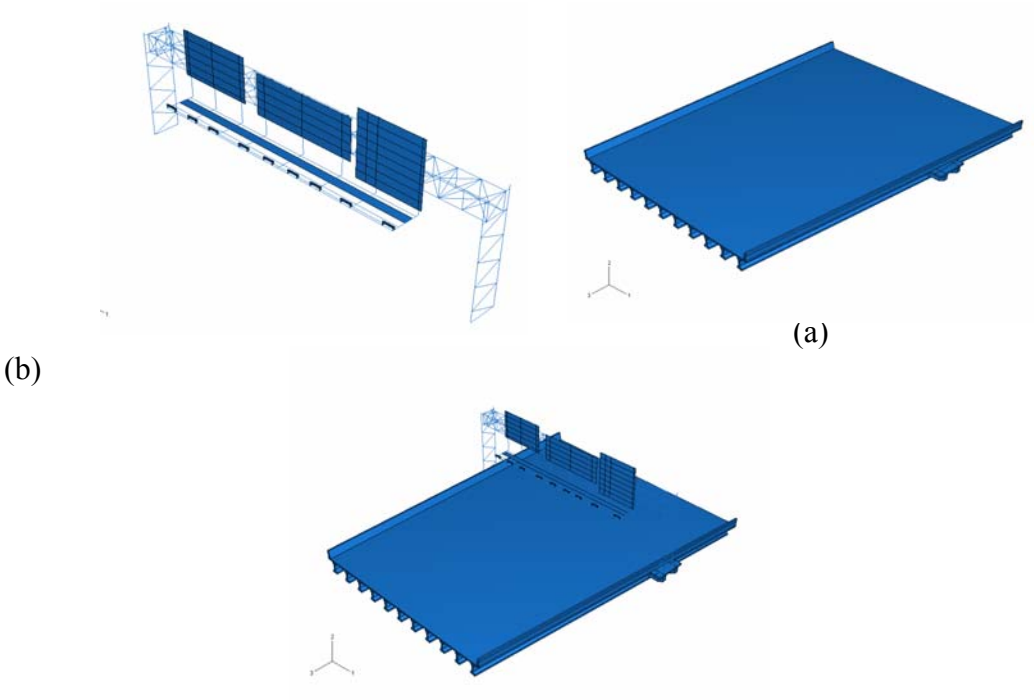

(a)

(b)

(c)

Figure 3.6 ABAQUS Models-(a) OSB 10633 Model; (b) Highway Bridge Model; (c) OSB 10633 and Highway Bridge Model

Table 3.2 Comparison of the Natural Frequencies of the Three Models

Mode / Model	OSB Mode	OSB Mode	OSB Mode	Highway Mode	Highway Mode	Highway Mode	Highway Mode	OSB Mode
Highway & OSB	2.29	2.90	3.10	3.83	3.98	4.18	4.27	4.42
Highway	N/A	N/A	N/A	3.84	4.00	4.18	4.30	N/A
OSB	2.76	2.96	3.36	N/A	N/A	N/A	N/A	4.53

Mode / Model	OSB Mode	Highway Mode	OSB Mode	OSB Mode	Highway Mode	Highway Mode	Highway Mode	Highway Mode
Highway & OSB	4.61	4.71	4.96	5.11	5.30	5.42	5.79	6.27
Highway	N/A	4.67	N/A	N/A	5.28	5.44	5.77	6.27
OSB	4.53	N/A	5.03	5.03	N/A	N/A	N/A	N/A

The first line in Table 3.2 is the modal frequencies for the model which included both the sign and highway bridges. The second row is the frequencies for the highway bridge alone at the indicated modes and the third row is the frequencies for the sign bridge alone at the indicated modes. The first three modes of the highway and OSB model correspond to the first three modes found in the analysis of the OSB alone. The slightly lower frequencies for the combined model are likely due to the added mass of the bridge and flexible support it provides for the OSB. The next 4 modes are essentially modes that involve the deflection of the highway bridge. The inclusion of the sign bridge does not significantly change the frequencies. The measured frequencies are generally lower than the values in Table 3.2. The existence of vehicles on the highway bridge during field tests increases the mass of the bridge structure which lowers the measured frequencies of vibration.

The conclusions from this analysis are:

1. The highway bridge affects the OSB's natural frequencies, especially the first mode of OSB vibration.
2. The OSB does not change the behavior of the highway bridge due to its relatively small weight.
3. The bare highway bridge model, as well as the model with the OSB mounted, shows that there is no pure "bending" mode of the highway bridge.
4. The flared geometry of the highway bridge influences the behavior of the highway bridge. The first four mode frequencies of the highway bridge are very close to each other, about 0.2 Hz between adjacent modes, and are combined flexural and torsional modes of the bridge.

3.2.2 Increase of Member Size

One of the possible solutions to the vibration problem is to increase the stiffness of OSB by increasing member size, which in turn will increase the natural frequencies of the OSB. Finite element models with increased members were calculated and the results listed in Table 3.3.

Table 3.3 Natural Frequencies of Original OSB and Strengthened OSB

Model	Natural Frequencies (Hz)				
	1st mode	2nd mode	3rd mode	4th mode	5th mode
Original model	**2.76**	**2.96**	**3.36**	**4.53**	**5.03**
25% increase in members	2.89	3.11	3.54	4.65	5.20
50% increase in members	2.98	3.23	3.69	4.73	5.32

These results did not show a significant change in the modal frequencies of the OSB. This suggests that the vibration problem will not be solved by simply increasing the member size. The horizontal truss depth must be increased to effectively increase the stiffness. The L frame connected to the sign and supporting the walkway and lights must also be stiffened.

3.2.3 Pluck Test Simulation

Pluck tests were done on site to determine the natural frequencies of the sign bridge. The weight was put at the mid-span position of the lower back chord and then released. Figure 3.7 shows the measured vertical acceleration at the truss mid-span within 4 seconds after pluck and the frequency analysis of the data. This test was simulated with the finite element model. The model does not include the highway bridge. The result of the finite element analysis is shown in Figure 3.8. The peak calculated response at 4.5 Hz is very close to the 4.25 Hz peak in the measured response. A smaller peak at 3.2 Hz is also evident in both the measured and calculated response.

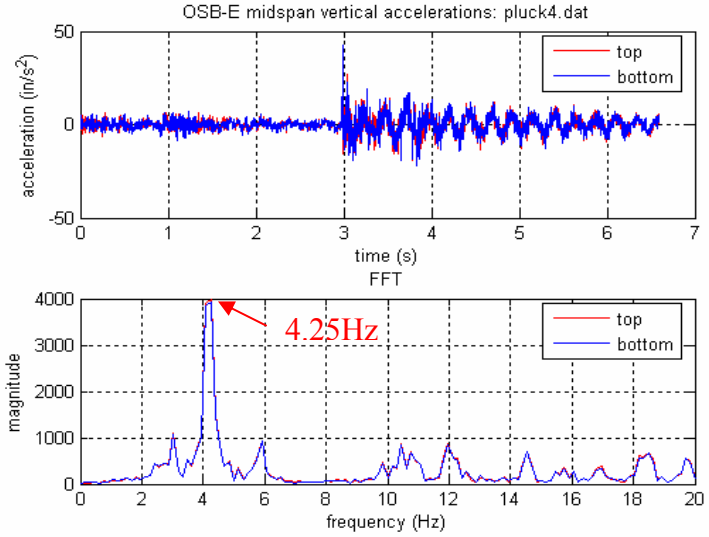

Figure 3.7 Field Pluck test results

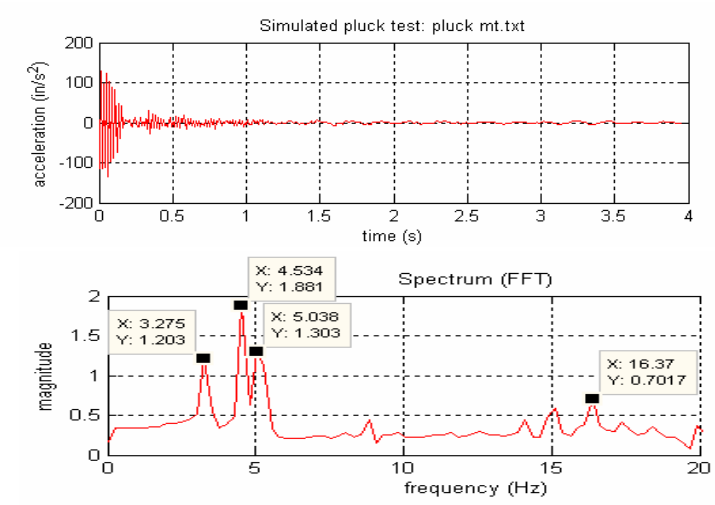

Figure 3.8 ABAQUS Simulated Pluck Test Results

3.2.4 Dynamic Response Analysis

Two time series, tests 18 and 1, acceleration data that were recorded by the accelerometers attached to the highway bridge were used to excite the overhead sign bridge finite element model. The maximum stress range and magnitude of vibration were predicted from this analysis. The acceleration inputs are shown in Figure 3.9 and the predicted ABAQUS response of the sign bridge at mid span is given in Figure 3.10. The stress range results were used to determine the location of the strain gages in the field tests. The displacements from this analysis were used as a base line to compare the influence of changes to the sign structure upon its dynamic response.

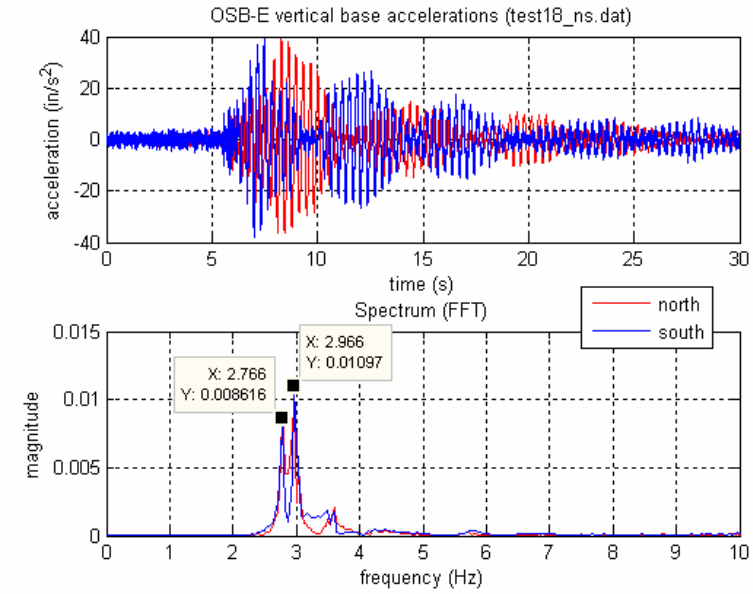

Figure 3.9 Time Series Acceleration Data Recorded Under Traffic (Test18)

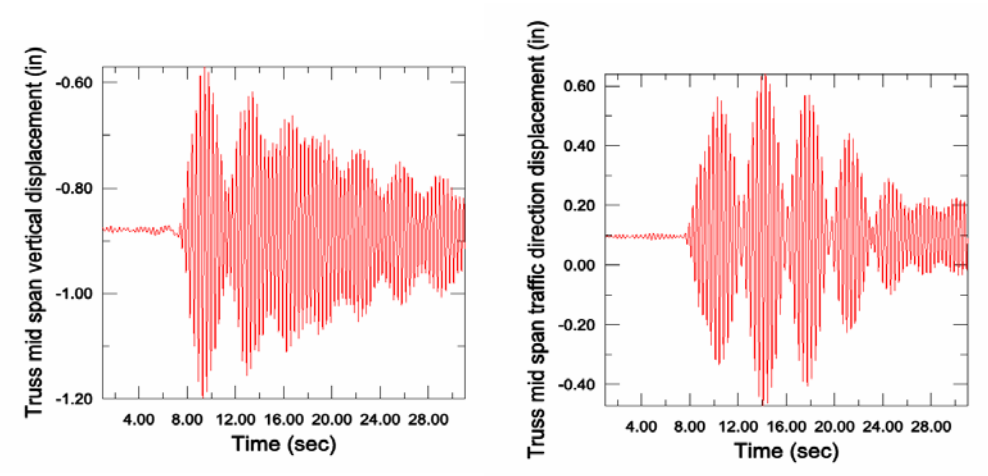

Figure 3.10 Predicted Mid-Span Displacement in Vertical and Traffic Direction under Vertical Acceleration Recorded in Test 18

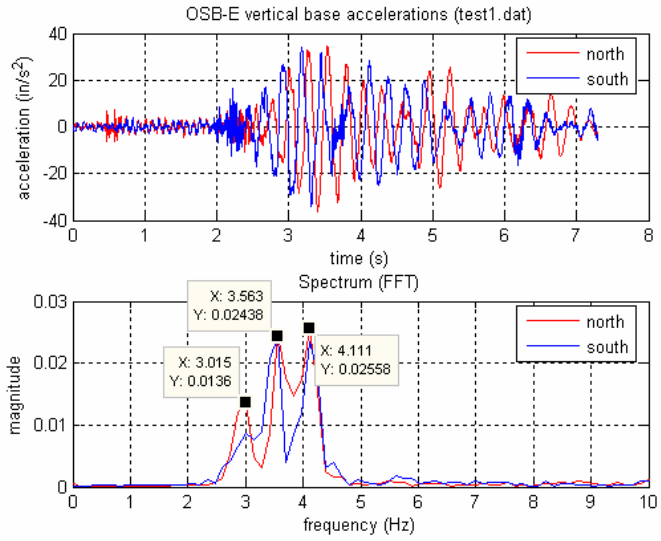

Figure 3.11 Time Series Acceleration Data Recorded Under Traffic (Test1)

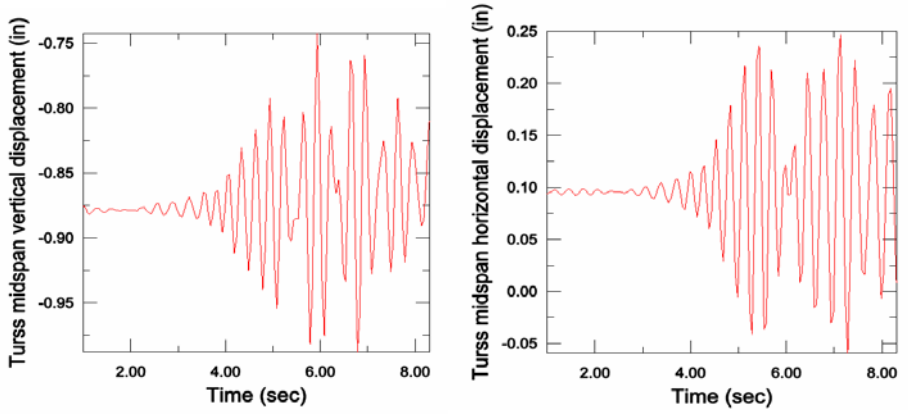

Figure 3.12 Predicted Truss Mid-Span Displacement in Vertical and Traffic Direction under Vertical Acceleration Recorded in Test 1

The measured accelerations in Test 1 are shown in Figure 3.11 and the predicted response of the sign bridge to these measured accelerations is shown in Figure 3.12. The sign bridge responses to both of the acceleration records show a beat frequency caused by the closeness of the natural frequency of the highway bridge and the OSB.

3.2.5 Dynamic Response Analysis without the Horizontal Arms of Sign Frame

A time series analysis using the same measured bridge acceleration records were performed with horizontal arms of the sign frame removed along with the attached lights and walkway. This was done since in the future the lights will no longer be required due to an improvement the sign reflectivity and it was suspected that removal of this mass would reduce the response of the OSB. The revised sign bridge model is shown in Figure 3.13. The predicted responses are shown in Figure 3.14 and Figure 3.15. The response of the modified structure to the original structure is compared in Table 3.4.

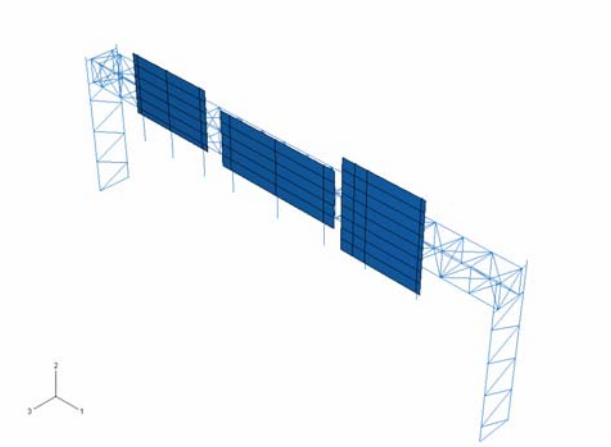

Figure 3.13 Revised Sign Bridge Model without Horizontal Arms, Lights and Walkway

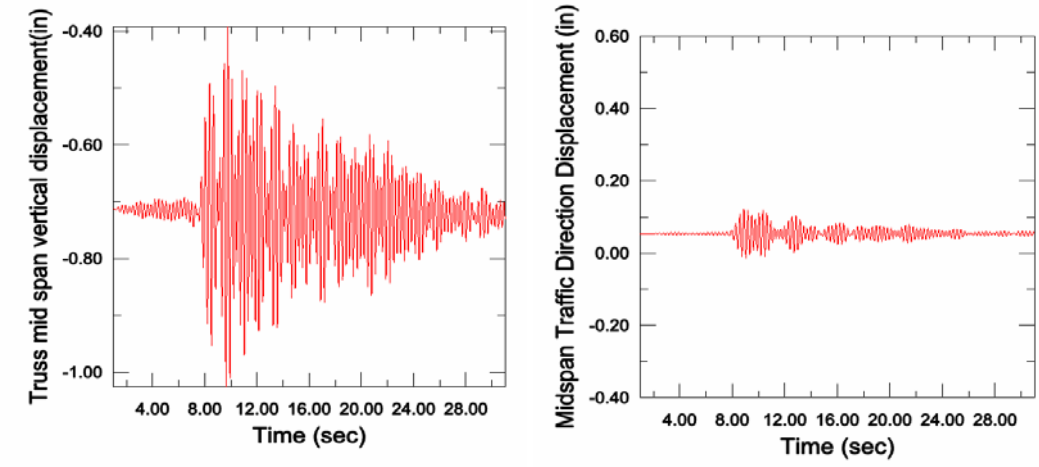

Figure 3.14 Predicted Truss Mid-Span Displacement in Vertical and Traffic Direction after Modification under Vertical Acceleration Recorded in Test 18

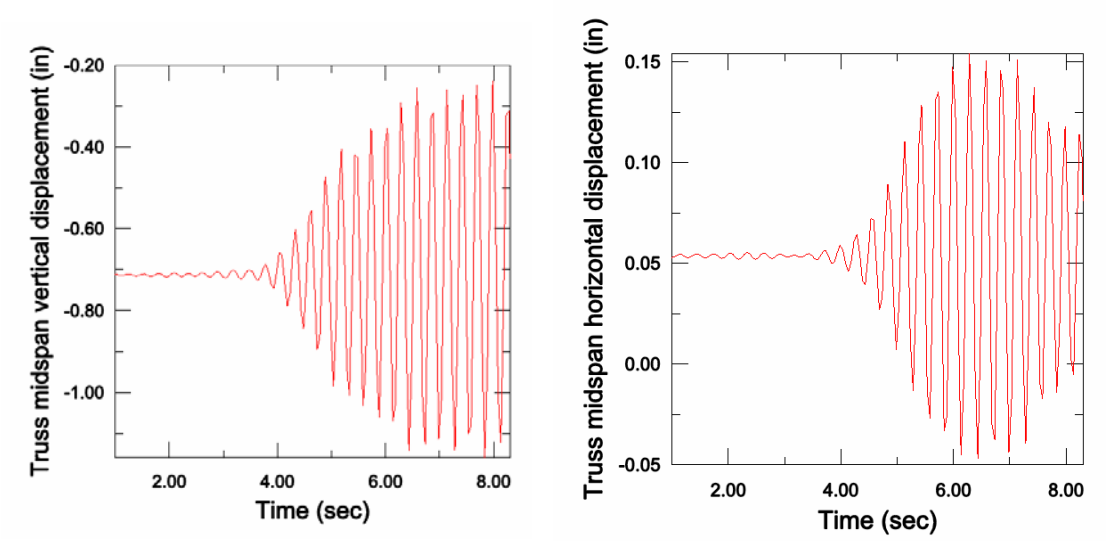

Figure 3.15 Predicted Truss Mid-Span Displacement in Vertical and Traffic Direction after Modification under Vertical Acceleration Recorded in Test 1

Table 3.4 Comparison of Response Magnitude of Original and Modified Structures to Recorded Base Accelerations

Input Acceleration	Maximum Acceleration (in/sec^2)	Major Frequency (Hz)	Original Structure Response Magnitude (in)		Modified Structure Response Magnitude (in)	
			Vertical	Horizontal	Vertical	Horizontal
Test 18	40	2.77; 2.97	0.60	1.00	0.60	0.10
Test 1	33	3.56; 4.11	0.25	0.30	0.95	0.20

The recorded vertical accelerations at the base of the OSB have different dominate frequencies due to the amount and distribution of traffic on the bridge. The predominant frequencies in the measured data vary from 2.5Hz to 5.0Hz. When the data from test18 was used to excite the sign bridge model, the horizontal direction dynamic response of the modified structure was drastically reduced while the vertical response did not change. When the accelerations from test1 are input into the model, the modified structure has a slightly reduced horizontal response but an increased vertical response. The elimination of dynamic excitation of the OSB cannot be prevented by removal of the walkway and lights. However, the removal of walkway and lights does reduce the vibrations in some frequencies and overall should reduce the incidents of noticeable OSB movement.

3.3 Analysis of OSB-W

3.3.1 Natural Frequency Analysis

Four finite element analysis models were analyzed as shown in Figure 3.16. One model had no sign mounted which matches the conditions of the field tests and a second model included a representation of the sign that was removed from the actual sign bridge prior to the field tests. The highway bridge is also modeled with an overhead sign bridge mounted on it to determine the interaction between the highway bridge and the OSB.

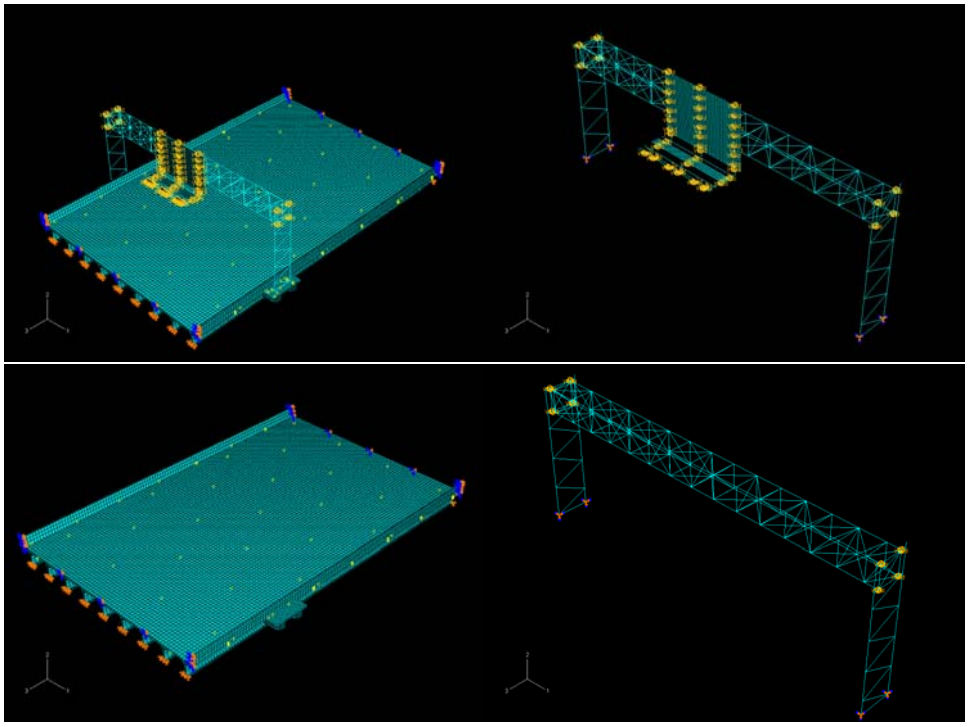

Figure 3.16 ABAQUS Models of OSB-W

The modal frequencies of the models are given in Table 3.5. The mode shapes are given in Appendix B. The inclusion of the sign structure reduced the natural frequency of the structure.

Table 3.5 Comparison of the Natural Frequencies of the Two Models

Mode / Model	OSB Mode (Sideway)	OSB Mode (Bending)	OSB Mode (Bending)	Highway Mode	Highway Mode	Highway Mode	Highway Mode
Highway & OSB	3.54	4.11	5.11	5.39	5.44	5.58	5.62
Highway	N/A	N/A	N/A	5.36	5.42	5.58	5.72
OSB with sign panel	3.95	4.18	5.29	N/A	N/A	N/A	N/A
OSB without sign panel	4.54	6.71	7.83	N/A	N/A	N/A	N/A

Mode / Model	Highway Mode	Highway Mode	Highway Mode	Highway Mode	Highway Mode	OSB Mode
Highway & OSB	5.89	5.96	6.22	6.40	6.72	7.10
Highway	5.89	5.99	6.18	6.40	6.71	N/A
OSB with sign panel	N/A	N/A	N/A	N/A	N/A	7.03
OSB without sign panel	N/A	N/A	N/A	N/A	N/A	14.74

3.3.2 Dynamic Response Analysis

Time series acceleration data recorded by the accelerometers attached to the highway bridge were used to excite the overhead sign bridge model. The acceleration inputs are shown in Figure 3.17 and the predicted response of the sign bridge at mid span is shown in Figure 3.18. The displacements from this analysis were used as a base line to compare the influence of changes to the sign structure upon its dynamic response.

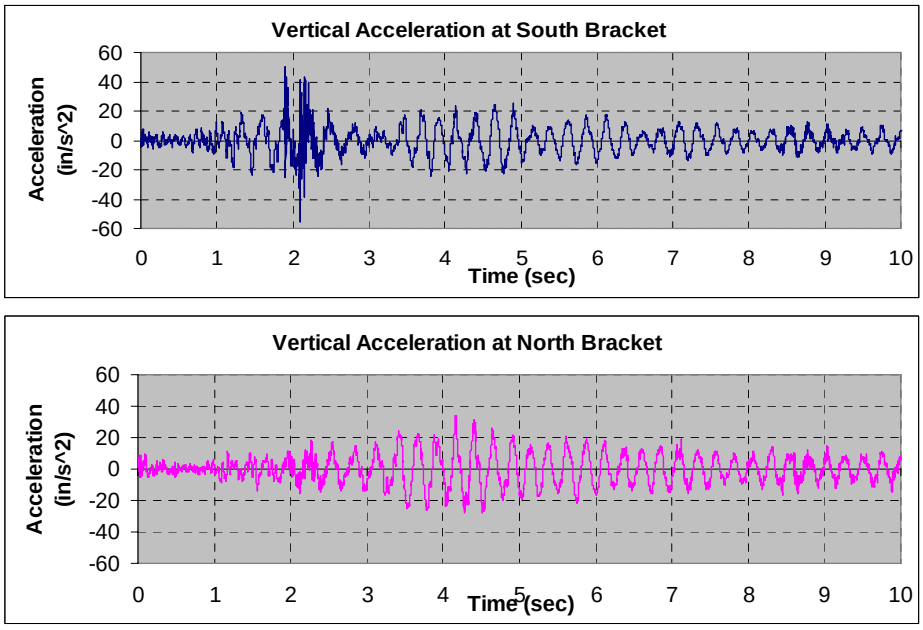

Figure 3.17 Time Series Acceleration Data Recorded Under Traffic

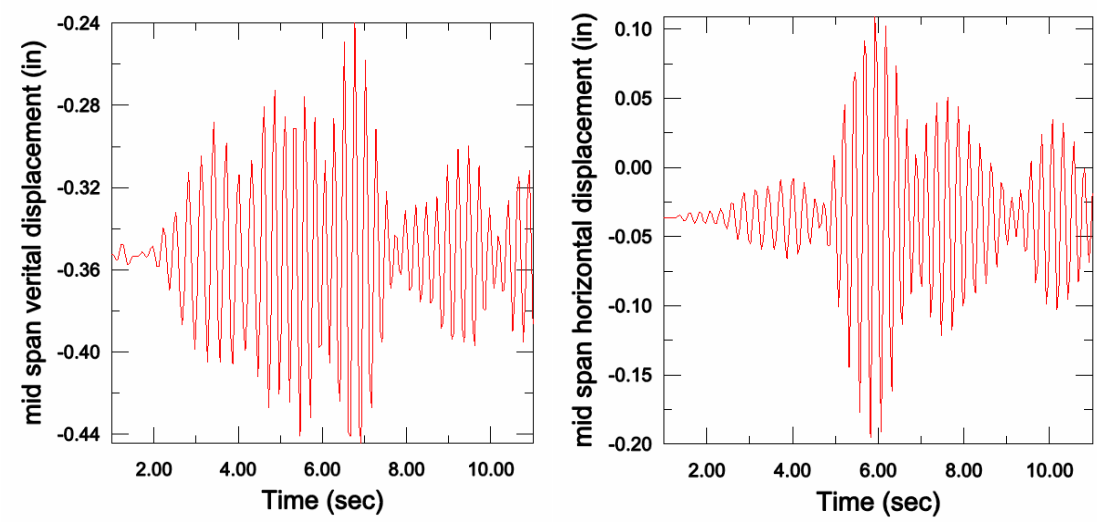

Figure 3.18 Predicted Truss Mid-Span Displacement in Vertical and Traffic Direction OSB-W

3.3.3 Dynamic Response Analysis without the Horizontal Arms of Sign Frame

The response of the modified sign bridge shown in Figure 3.19 is plotted in Figure 3.20 and can be compared the results in Figure 3.14 of the OSB with the horizontal arms. The maximum vertical displacements in the two models are comparable but the displacements damp out quickly in the OSB without the support. The horizontal displacement of the structure without the walkway and lights is negligible. Clearly, removal of these items from the structure will reduce the dynamic oscillation of the OSB.

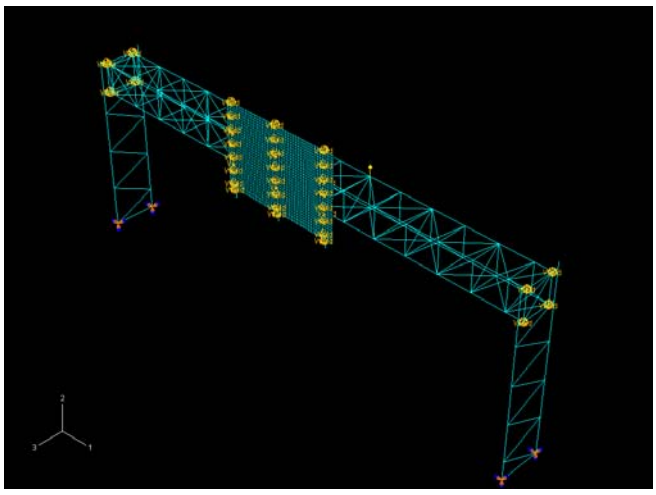

Figure 3.19 Revised OSB-W Model without Horizontal Arms, Lights and Walkway

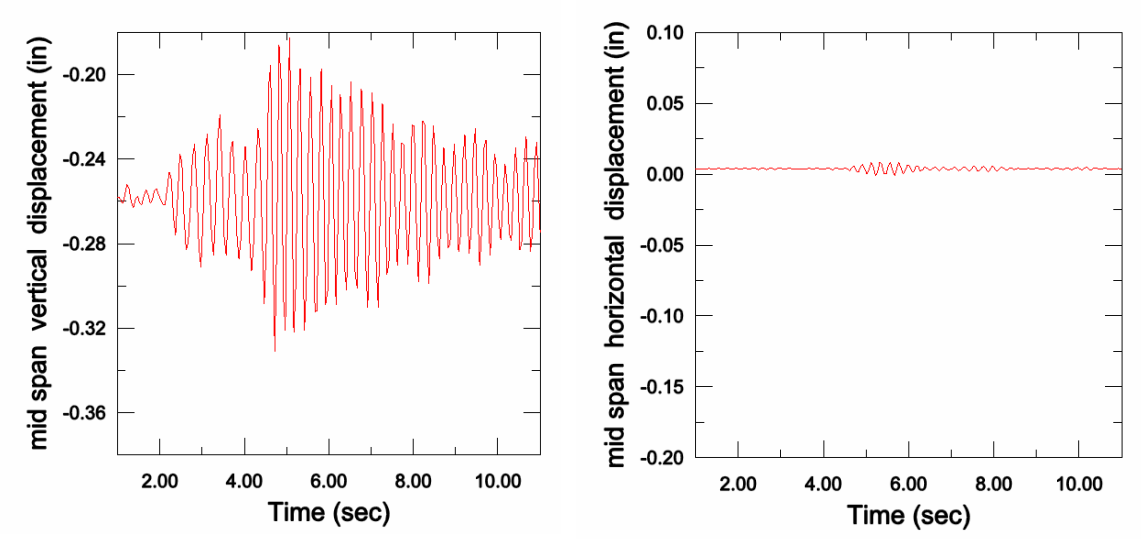

Figure 3.20 Predicted Truss mid Span Displacement in Vertical and Traffic Direction after Modification OSB-W

Chapter 4

Summary and Recommendations

4.1 Summary

The field studies found that the vibrations of the overhead sign bridges were due to traffic induced vibrations of the supporting highway bridges. It was observed that the signs started vibrating before a vehicle passed under the sign bridge. Both the OSB-W and OSB-E were excited by vehicles not in the lanes under signs, therefore eliminating gust loads from the vehicles as a source of the observed sign vibrations.

The fundamental frequencies of the bridges were between 4 and 5 Hz. The fundamental frequencies of OSB-E, which had signs mounted, was between 3.2 and 4.1 Hz which is lower than the bridge. Even though natural frequencies of the two structures differed, the vibration of the bridge produced significant movement of the sign bridge. OSB-W, which was a shorter span sign bridge with no signs on it, had a higher natural frequency than the bridge and had a much smaller measured vibration amplitude. The frequency of vibration of the highway bridge appeared to be a function of the number of vehicles present on the bridge, which would increase the vibrating mass, and the lateral location of the vehicle on the bridge. Torsional modes of bridge vibrations occurred when the truck was in the outside lanes of the bridge.

Fatigue of the sign bridge structure was not found to be of concern. The calculated and measured stress ranges in the bolted truss members and the welds on the vertical supports were too small to cause fatigue problems. The welds connecting the two legs of the small W shape L brackets, which are used to mount the sign and support the walkway and lights in front of the sign, were found to be of concern. The maximum stress range measured was from 9.6 to 13.9 ksi with an effective stress range of 1.9 to 2.2 ksi. The expected minimum fatigue life would be less than 10 years. The analytical study indicated that removal of the cantilever portion of the L bracket along with the walkway and lights reduced the dynamic oscillations of the OSB for some modes of highway bridge vibration.

4.2 Recommendations

1. Remove the horizontal cantilever portion of the wide flange L brackets. This will reduce the vibrations in the OSB and eliminate the fatigue prone weld detail at the connection of the vertical and horizontal legs of the bracket.
2. Tighten all bolts on the sign bridge using the turn of the nut method. Loose bolts have been found in an inspection prior to this study. The movement of the sign bridge will loosen bolts unless they are properly tightened.
3. Mount the sign as close as possible the bridge pier to reduce the movement of the highway bridge at location of the OSB.

Appendix A

Model Shapes OSB-E

1st Mode: (OSB mode)

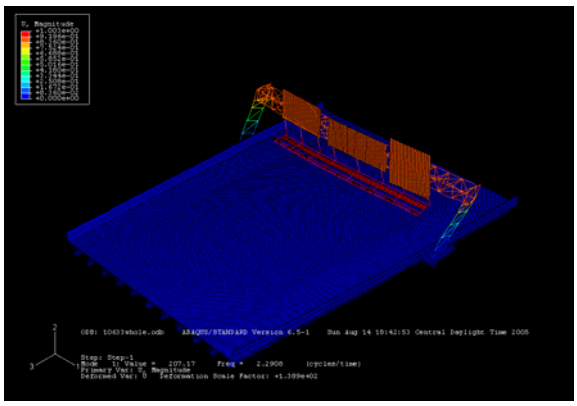

2.29 Hz

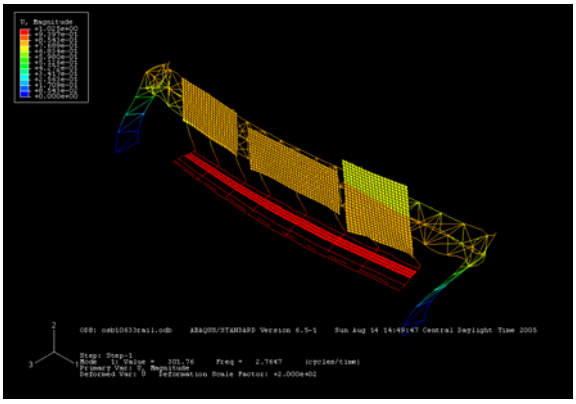

2.76 Hz

2nd Mode: (OSB mode)

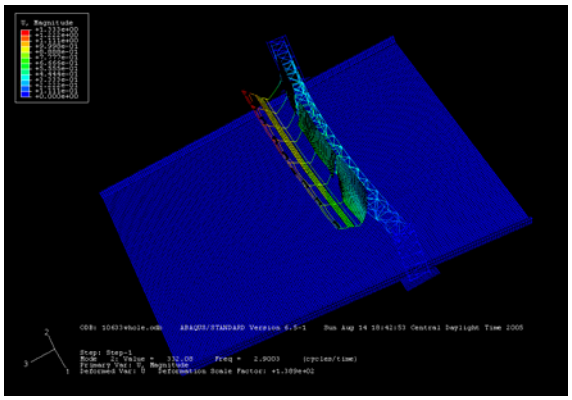

2.90 Hz

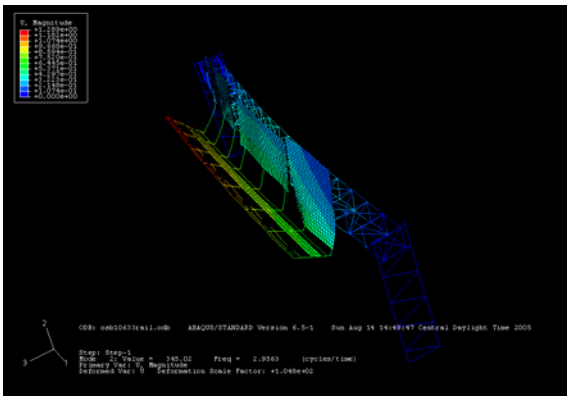

2.95 Hz

3rd Mode: (OSB mode)

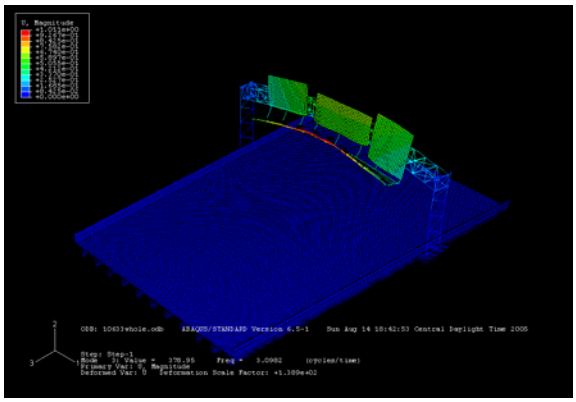

3.10 Hz

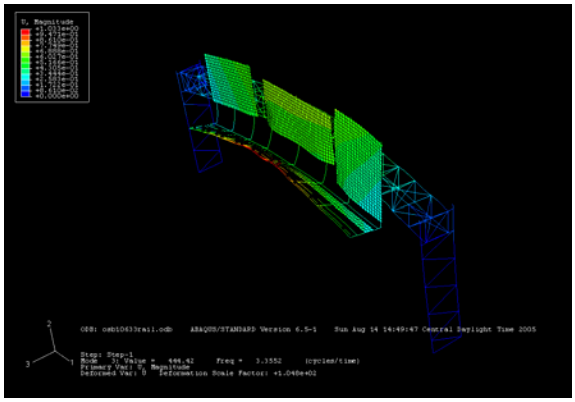

3.36 Hz

4th Mode: (Highway bridge mode)

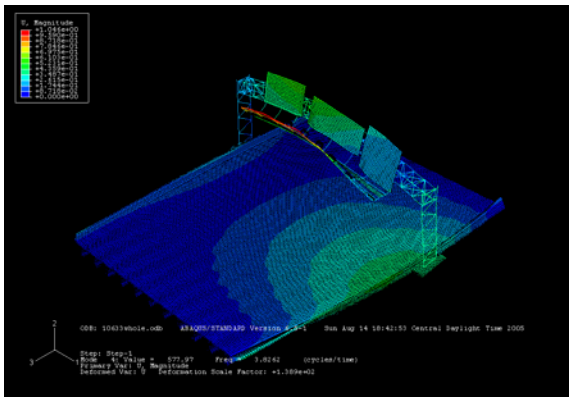

3.83 Hz

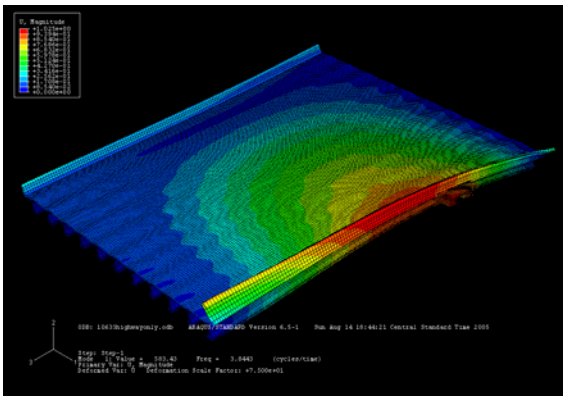

3.84 Hz

5th Mode: (Highway bridge mode)

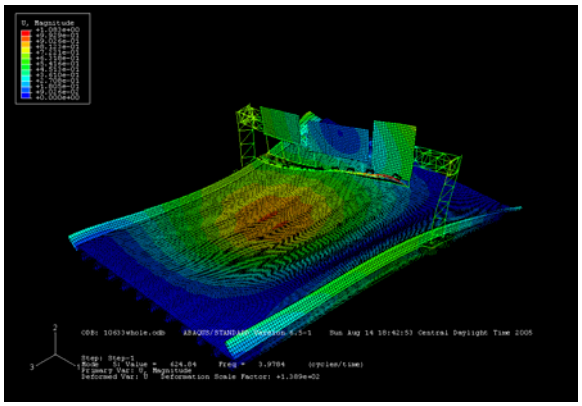

3.98 Hz

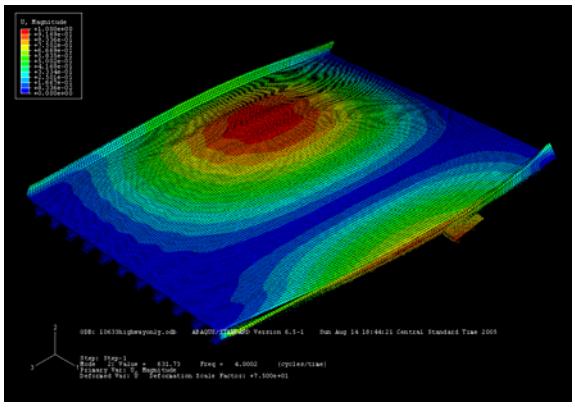

4.00 Hz

6th Mode: (Highway bridge mode)

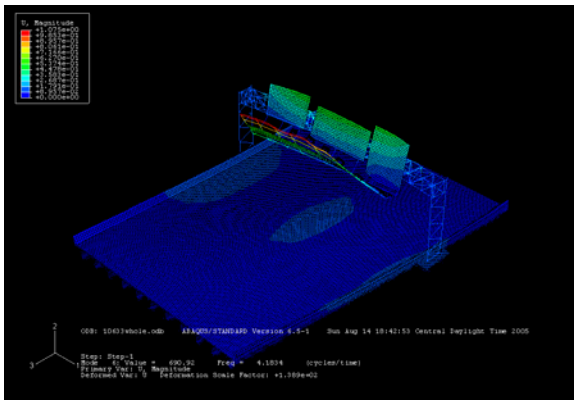

4.18 Hz

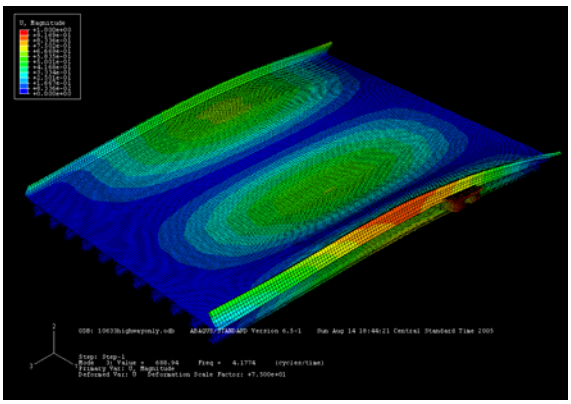

4.18 Hz

7th Mode: (Highway bridge mode)

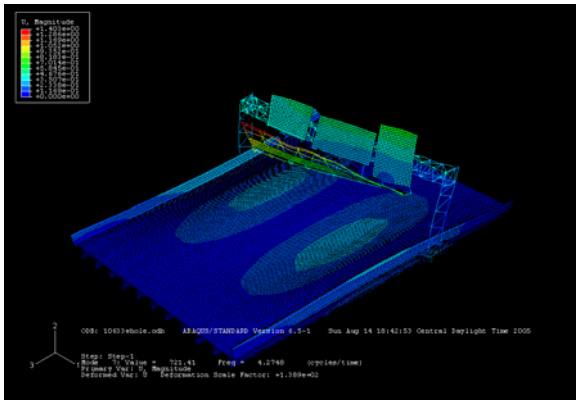

4.27 Hz

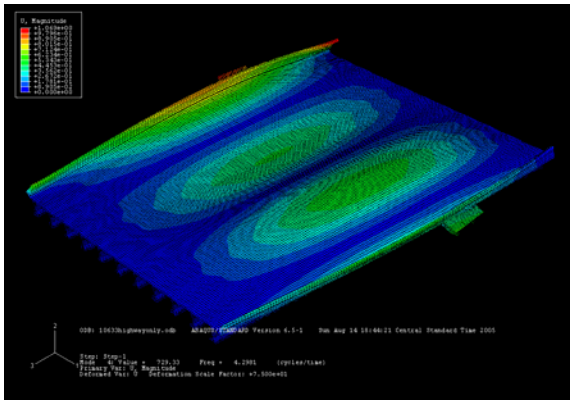

4.30 Hz

8th and 9th Mode: (Single OSB mode is broken into two modes)

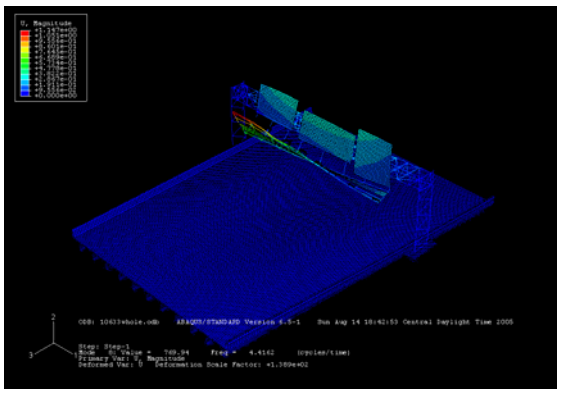

4.42 Hz

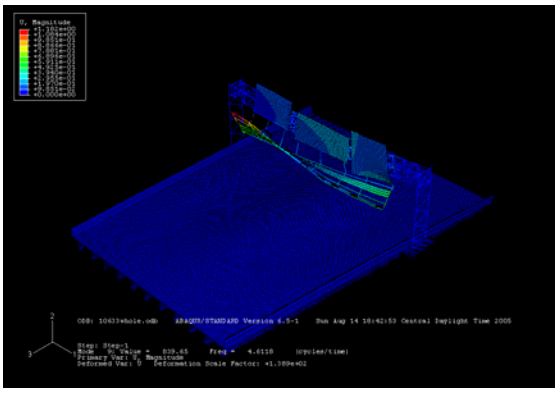

4.61Hz

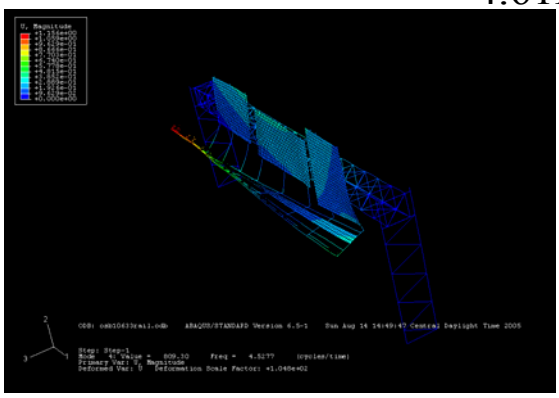

4.53 Hz

10th Mode: (Highway bridge mode)

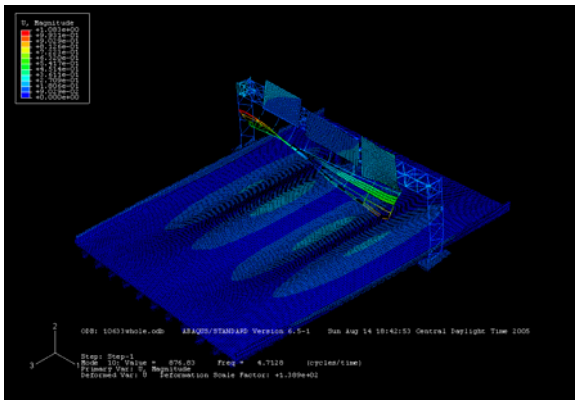

4.71 Hz

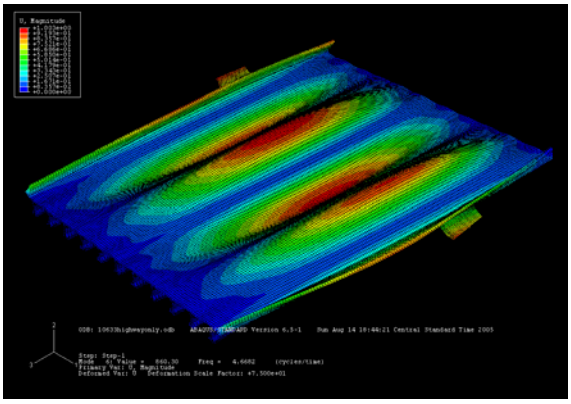

4.67 Hz

11th and 12th Mode: (Single OSB mode is broken into two modes)

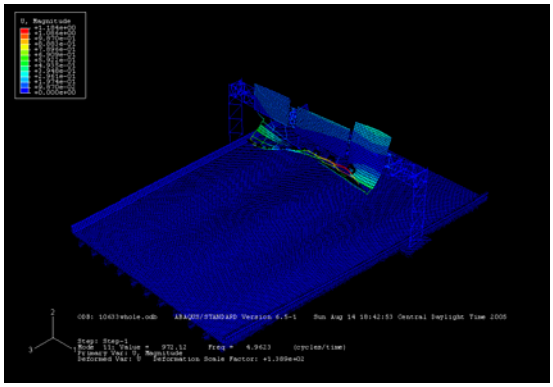

4.96 Hz

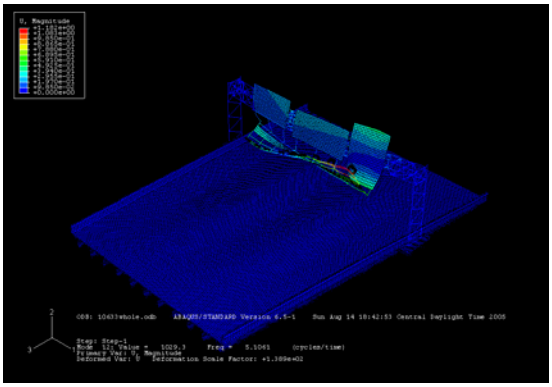

5.11

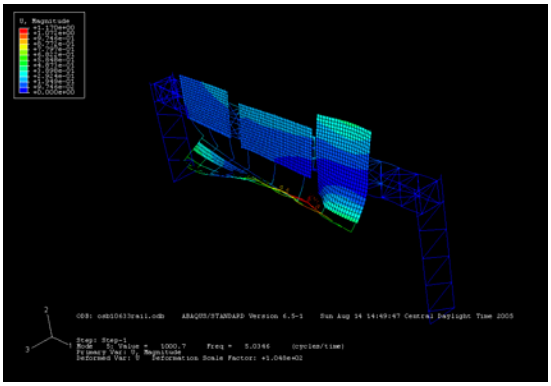

5.03 Hz

13th Mode: (Highway bridge mode)

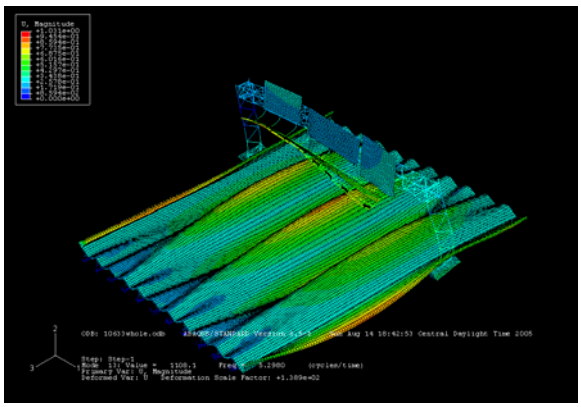

5.30 Hz

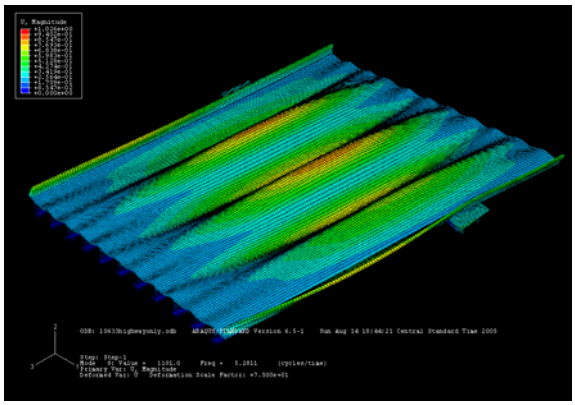

5.28 Hz

14th Mode: (Highway bridge mode)

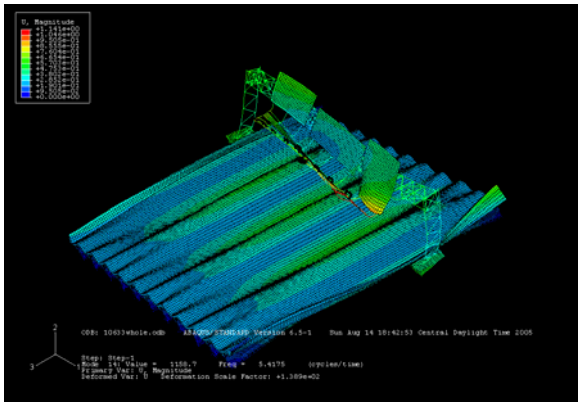

5.42 Hz

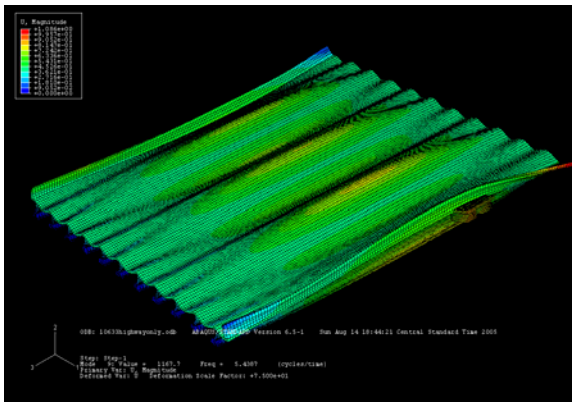

5.44 Hz

15th Mode: (Highway bridge mode)

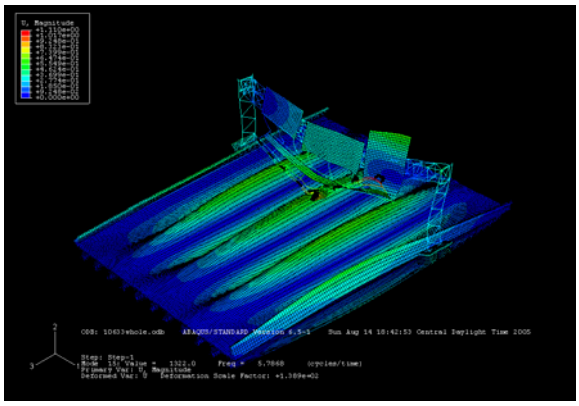

5.79 Hz

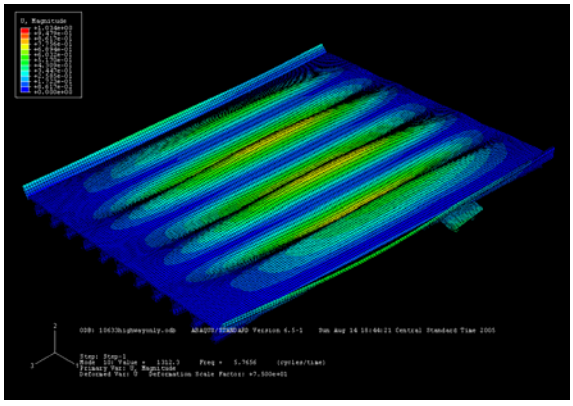

5.77 Hz

16th Mode: (Highway bridge mode)

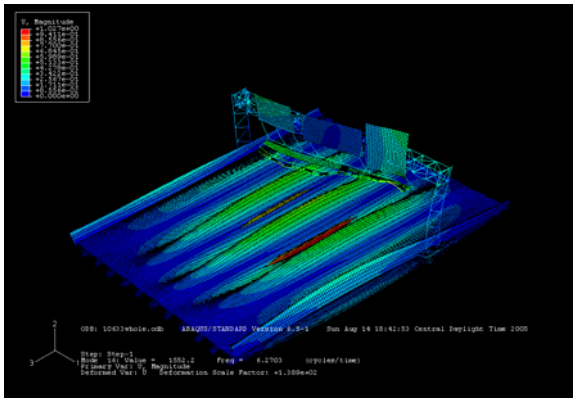

6.27 Hz

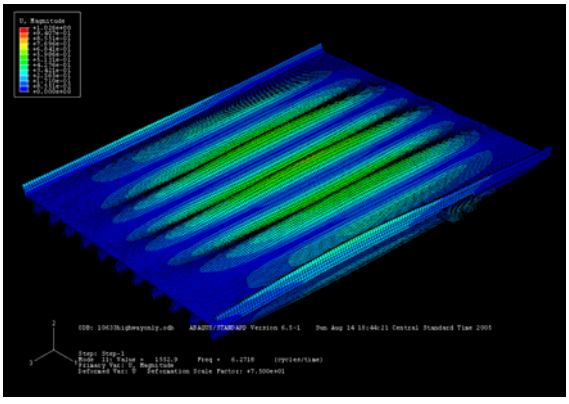

6.27 Hz

Appendix B

Mode Shapes OSB-W

1st Mode:

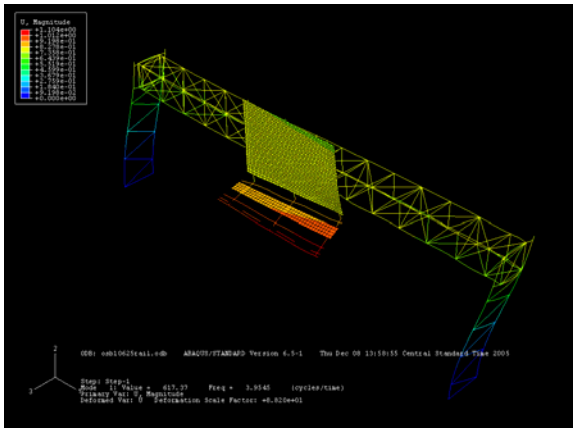

3.95 Hz

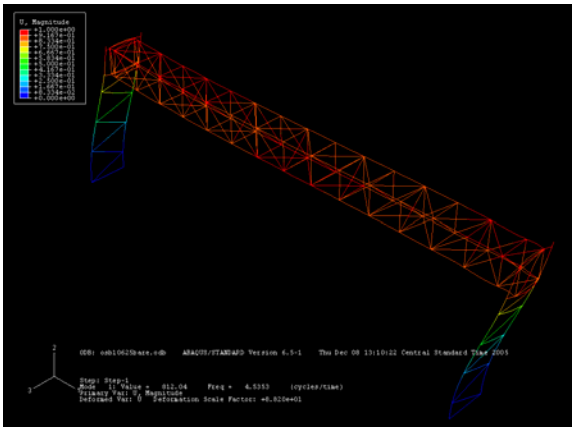

4.54 Hz

2nd Mode:

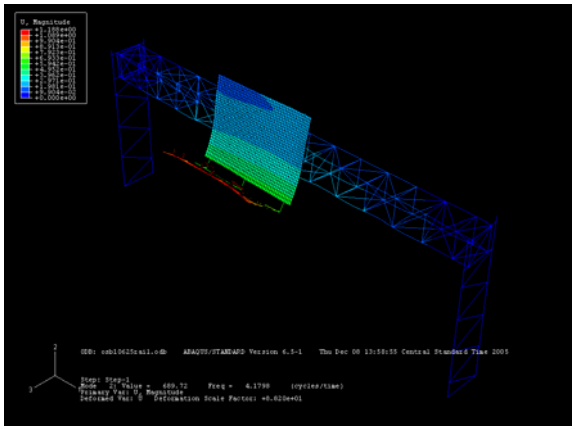

4.18 Hz

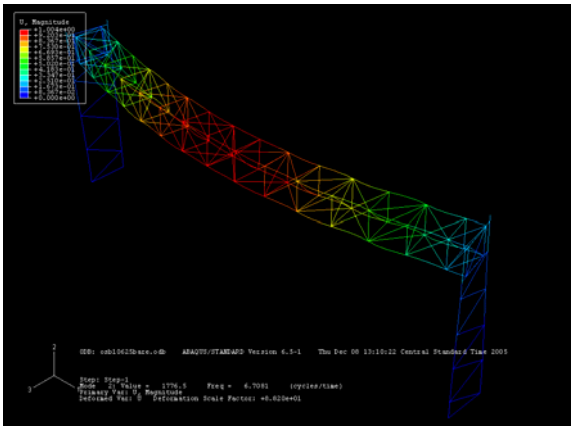

6.71 Hz

3rd Mode:

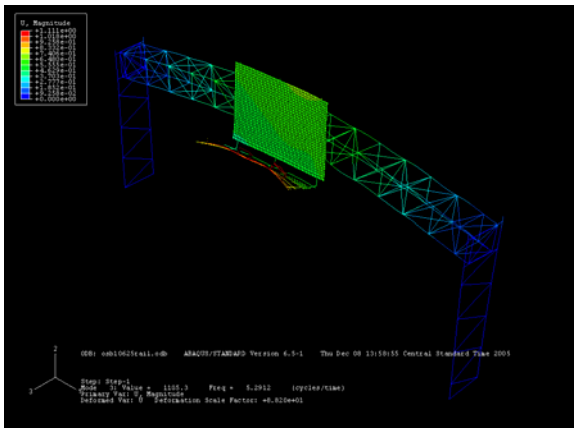

5.29 Hz

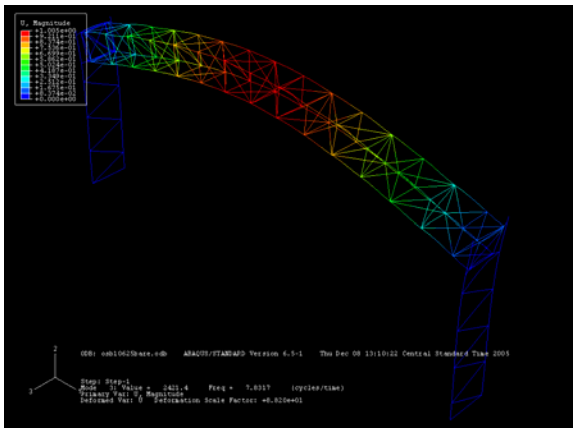

7.83 Hz

4th Mode:

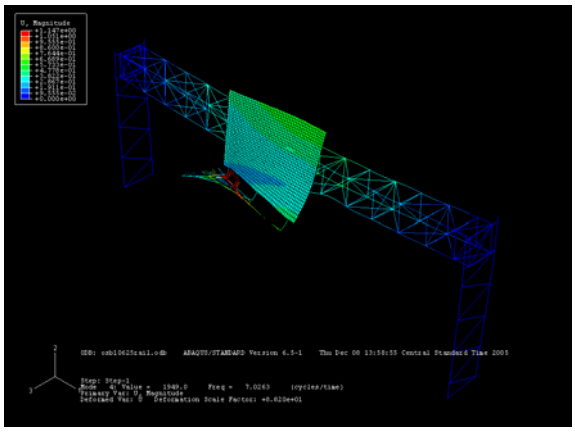

7.03 Hz

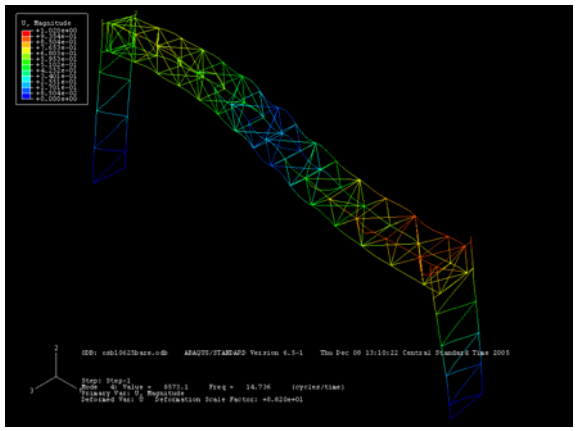

14.74 Hz

5th Mode:

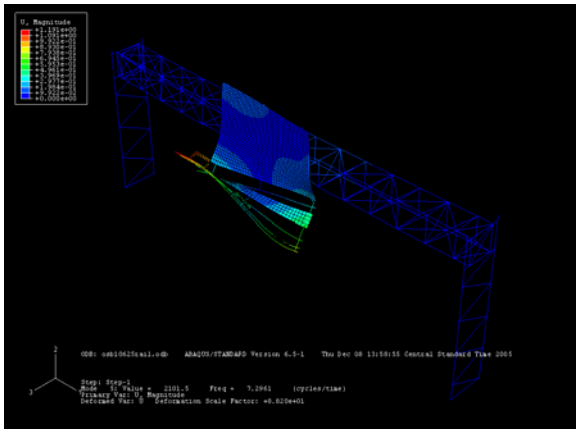

7.30 Hz

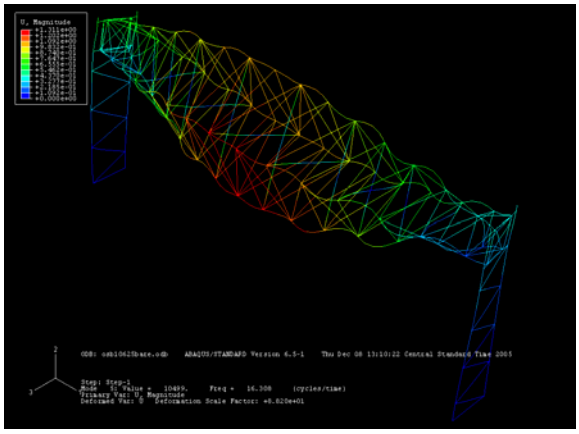

16.31 Hz

6th Mode:

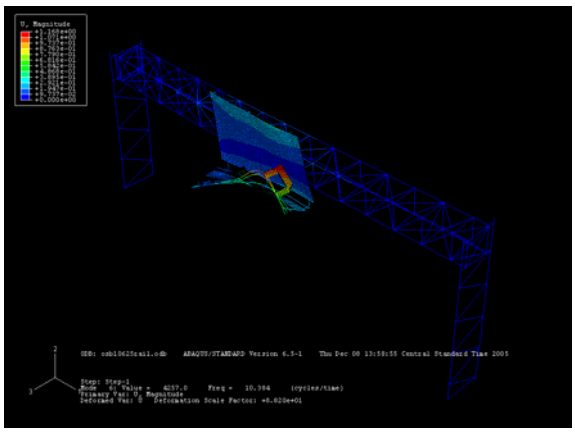

10.38 Hz

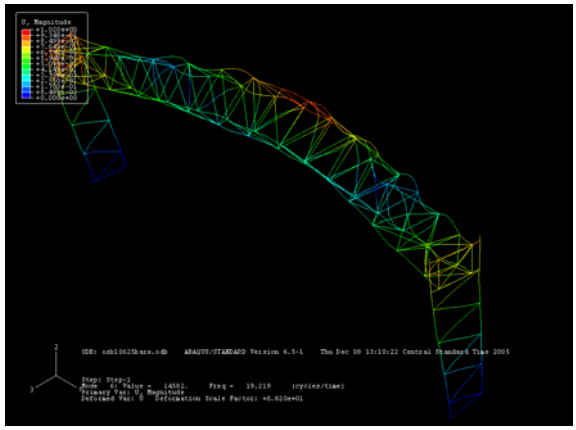

19.22 Hz

7th Mode:

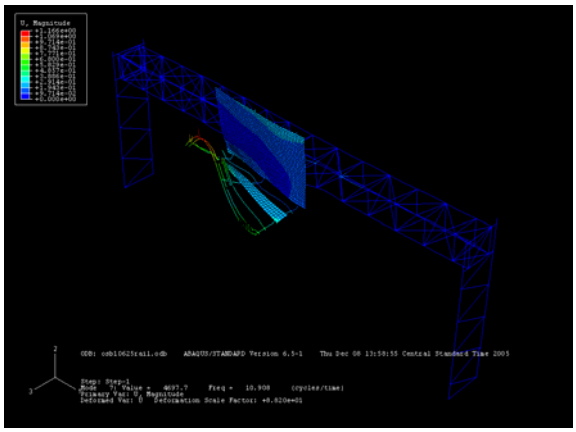

10.91 Hz

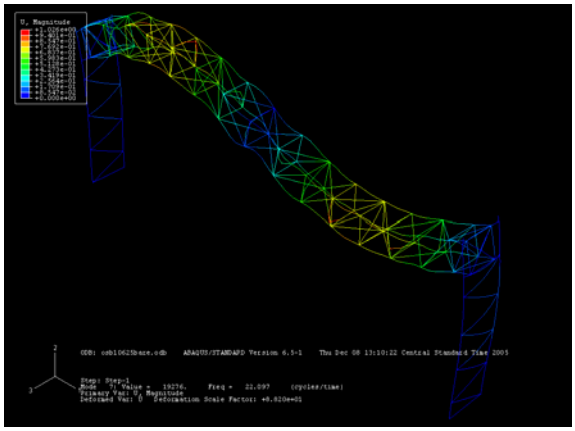

22.10 Hz

8th Mode:

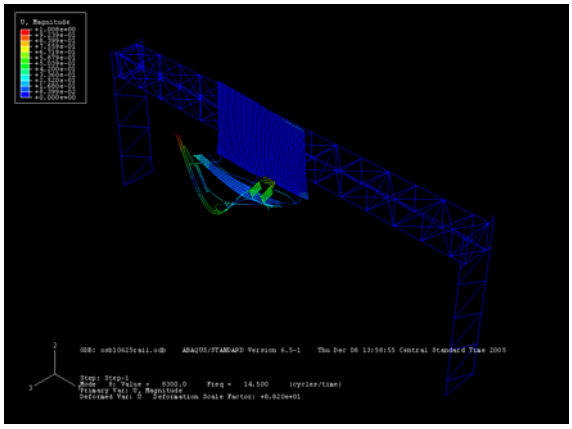

14.50 Hz

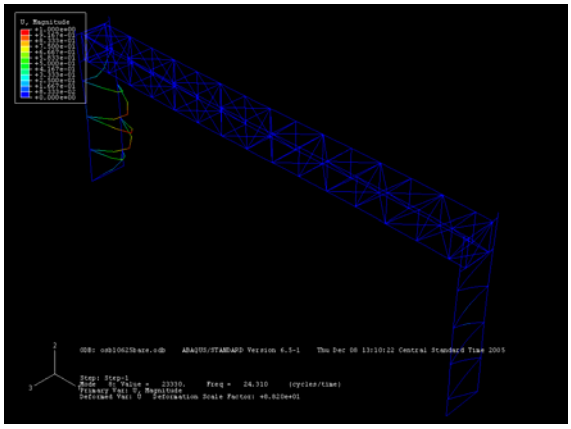

24.31Hz